14 (2022) 100144

Contents lists available at ScienceDirect

International Journal of Thermofluids

journal homepage: www.elsevier.com/locate/ijtf

Numerical analysis of performance uncertainty of heat exchangers operated with nanofluids

B. Kamenik [a], E. Begum Elcioglu [d], A. Turgut [c], R. Mondragón [b], L. Hernandez Lopez [b], J.P. Vallejo [g], L. Lugo [f], M.H. Buschmann [e], J. Ravnik [a,*]

[a] Faculty of Mechanical Engineering, University of Maribor, Smetanova 17, SI-2000, Maribor, Slovenia
[b] Departamento Ingeniería Mecánica y Construcción, Universitat Jaume I, Castellón, Spain
[c] Department of Mechanical Engineering, Dokuz Eylul University, Izmir, Turkey
[d] Department of Mechanical Engineering, Eskişehir Technical University, Eskişehir, Turkey
[e] Institut fuer Luft- und Kaeltetechnik, Dresden, Germany
[f] CINBIO, Universidade de Vigo, Grupo GAME, Departamento de Física Aplicada, 36310 Vigo, Spain
[g] Centro Universitario de la Defensa en la Escuela Naval Militar, Plaza de España, s/n, 36920 Marín, Spain

ARTICLE INFO

Keywords:
Nanofluid
Heat exchanger
Figure of merit
Stochastic collocation method
Statistical analysis
Correlation analysis

ABSTRACT

In this paper, we analyse the performance of two types of heat exchangers with nanofluid as the working fluid in turbulent flow regime ($Re \approx 4,000–180,000$). Based on the experimental uncertainty of the thermophysical properties of the nanofluids, we use the Stochastic Collocation Method in combination with a deterministic simulation programme to estimate the expected value and variance of the targeted engineering results. We find that the uncertainty in the thermal conductivity of the nanofluid has the largest impact on the uncertainty in the heat exchanger performance, while the uncertainty in the density can be neglected. The uncertainties in the Nusselt number, friction factor and several figures of merit are smaller than the change in these performance estimators due to a change in nanoparticle concentration. Predictions for heat exchanger performance agree much better with experimental data when used with empirical heat transfer correlations developed specifically for nanofluids than with the general Gnielinski correlation developed for pure fluids.

We also perform a correlation analysis of the relationships between heat exchanger performance enhancement and pressure drop to show that they are strongly correlated. We find that the relationship between the concentration of nanoparticles and the Nusselt number is statistically insignificant. The $Re - Nu$ relationship is significant, indicating the importance of flow conditions. The correlation between nanoparticle concentration and friction factor is significant and strong. This result suggests that the optimisation of the thermal-hydrodynamic behaviour should be sought in a parameter other than the nanoparticle volume fraction.

1. Introduction

It has been more than two decades since Choi and Eastman [1] referred to nanoparticle dispersions in base fluid as nanofluids and highlighted the opportunities that could be brought by their high thermal conductivity. After more than two decades of experimental and numerical work [2–9], the advantages nanofluids offer are appreciated in a larger number of systems and settings, while their inherent challenges are also better understood. Such challenges include nanoparticle agglomeration and instability (including long-term) issues [10,11], uncertainties [11], nanofluid preparation [11] and the absence of standard preparation protocols [12], increased pumping power requirements [10], corrosion of components [10], and the need for performing systematic research [11], among others.

In order to better understand the magnitudes of the impacts these challenges present and to identify those that may be critical, mathematical tools are needed. Statistical analyses provide valuable information through parameter effect comparison (e.g., [13,14]), correlation analysis [15] (to observe the extent of association between variables) (e.g., [16,17]), prediction model development by regression analysis (e.g., [15,18,19]), among many others. In the statistical part of this work, we aim to perform a rigorous statistical assessment on nanofluid data via correlation analysis and variance analysis. We provide underlying

* Corresponding author.
E-mail addresses: blaz.kamenik@um.si (B. Kamenik), ebelcioglu@eskisehir.edu.tr (E.B. Elcioglu), alpaslan.turgut@deu.edu.tr (A. Turgut), mondragn@uji.es (R. Mondragón), lhernand@uji.es (L. Hernandez Lopez), jvallejo@uvigo.es (J.P. Vallejo), luis.lugo@uvigo.es (L. Lugo), Matthias.Buschmann@ilkdresden.de (M.H. Buschmann), jure.ravnik@um.si (J. Ravnik).

https://doi.org/10.1016/j.ijft.2022.100144
Received 9 December 2021; Received in revised form 18 February 2022; Accepted 21 February 2022
Available online 7 March 2022

Nomenclature

Latin symbols

C	Heat capacity rate [W/K]
CNT	Carbon nanotubes
c_p	Heat capacity, [J/kg K]
CP	Control point
Eu	Euler number [−]
F	Correction factor
FOM	Figure of merit
FTP	Full tensor product
GNP	Graphene nanoplatelets
h	Heat transfer coefficient, [W/m^2 K]
k	Thermal conductivity, [W/m K]
$\mathcal{L}$	Characteristic dimension, [m]
L, d, A	Length, diameter, area, [m], [m^2]
$LMTD$	Logarithmic mean temperature difference [K]
$\dot{m}$	Mass flow rate [kg/s]
Mo	Mouromtseff ratio [−]
n	Number of cases [−]
NTU	Number of transfer units [−]
Nu	Nusselt number [−]
OAT	One-at-a-time
P	PDF - probability density function
p	Significance value
Pe	Péclet number [−]
PEC	Performance Evaluation Criteria
Pr	Prandtl number [−]
$\dot{Q}$	Heat transfer rate [W]
Re	Reynolds number [−]
SCM	Stochastic collocation method
S	Sensitivity index
T	Temperature [°C]
U	Overall heat transfer coefficient [W/m^2 K]
u	Velocity [m/s]
ER	Energy ratio [−]
$\dot{V}$	Volumetric flow rate [m^3/ s]
var	Variance

Greek symbols

Δp	Pressure drop [Pa]
ϵ	Effectiveness
η	Overall energetic efficiency [−]
η_{tf}	Thermal performance factor [−]
μ	Dynamic viscosity, [Pa s]
μ_y	Expected value of parameter as a result of the stochastic collocation method
ϕ_v	Nanoparticle volume fraction [−]
ω	Uncertainty of a value [%]
ρ	Density, [kg/m^3], correlation coefficient
σ	Random variable
ξ	Friction factor [−]

Subscripts

ann	Annulus
avg	Average value
h	Hydraulic
in	Inlet
nf	Nanofluid
out	Outlet
par	Partial
w	Water
$wall$	Pipe wall

statistical assumptions, so that the reader can follow how the proper tests are selected and performed. In a system-specific way, the direct and indirect thermal performance indicators of nanofluids are studied using correlation analysis and variance analysis to assess which process variables correlate to the indicators more or exhibit a certain type of relation with the indicators. This is done with the aim of informing potential performance/system improvement strategies.

Most mathematical models used in engineering practice are deterministic. This means that, for a given set of input parameters, a simulation is performed that yields a single set of relevant quantities. Although the implementation of deterministic numerical techniques based on the mechanistic models leads to practical insight into the behaviour of the underlying phenomena, there are certain cases that cannot be solved by deterministic modelling alone.

The mathematical–physical model describing the flow and heat transfer processes in nanofluids is based on the model of nanofluid properties. These can be obtained via theoretical approaches [20] or via experimental work [21]. We observe a large variation in nanofluid properties obtained from experiments and models.

Any process is sensitive to a change in process conditions. If there is an additional sensitivity to the material and model parameters used in the computational model, the uncertainty from the input will inevitably be transferred to the output of interest, which in the case of nanofluid heat transfer are the temperature distribution and heat flux. To gain better insight into the quality of the computational results, the model input parameters, such as the properties of the nanofluid, should be considered as random variables and a corresponding computational uncertainty analysis [22] should be performed. The aim of this work is to propagate the experimentally determined uncertainty in nanofluid properties to the target engineering results, such as the heat transfer performance of a heat exchanger.

Traditionally, Monte Carlo type methods [23] have been used to capture the response of deterministic simulations to changes in input parameters. These methods have extremely slow convergence rates, which means that a very large number of deterministic simulations is required to obtain statistically relevant results. For more physically and numerically sophisticated models, of which computational fluid dynamics is a prime example, it is simply not possible to perform the needed number of simulations.

In contrast to the statistical approaches, non-statistical algorithms aim at representing the unknown stochastic solution as a function of random input variables. Among the various methods available in the literature, the Generalised Polynomial Chaos technique [24] based on spectral discretisation is one of the most commonly used. Its two variants are the Galerkin Stochastic Method and Stochastic Collocation Method (SCM) [25,26]. The intrusive nature of the Galerkin Stochastic Method requires a more sophisticated implementation, as new algorithms have to be developed. In contrast, the non-intrusive nature of the SCM allows the use of existing reliable deterministic models as black boxes in stochastic computations. Both approaches show fast convergence and high accuracy under different conditions. The combination of the non-intrusive sample-based nature of Monte Carlo simulations with the polynomial approximation of the output value characteristic of polynomial chaos methods has made stochastic collocation one of the most widely researched and applied stochastic approaches.

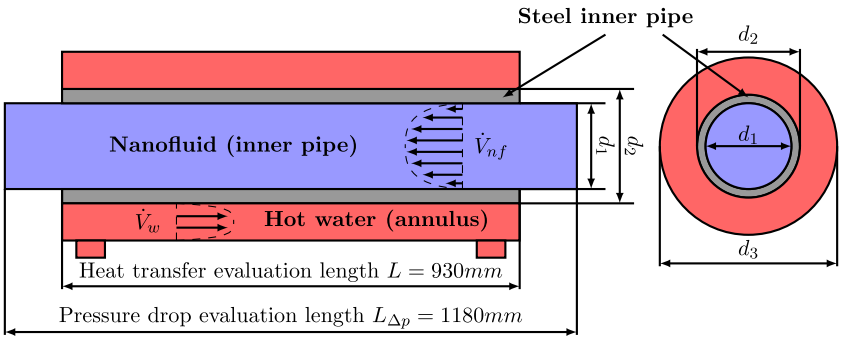

Fig. 1. Geometry of the studied pipe-in-pipe heat exchanger (Agromayor et al. [28]).

The use of the SCM thus makes it possible to conduct a sensitivity analysis [27], which examines how the outcomes of a system are related to and affected by its input parameters. In our research, the system in question is a heat exchanger modelled by a mathematical model that relates the experimental uncertainty of the nanofluid thermophysical properties as inputs to the output variables such as the Nusselt number, the heat transfer coefficient, and figures of merit. The analysis was performed for various nanofluids in two heat exchangers operating in turbulent flow regime ($Re \approx 4000 - -180{,}000$).

The paper is structured as follows: Section 2 presents the mathematical model for heat exchangers and the implementation of the SCM. Furthermore, it focuses on the statistical assessment of the relationships between nanofluid properties and performance indicators. Section 3 presents the results of the analysis, while Section 4 summarises the main conclusions.

2. Mathematical and statistical models of heat exchanger performance

We consider two designs of a heat exchanger where we demonstrate how uncertainties in the thermophysical properties of nanofluids affect the engineering estimate of the transfer performance of a heat exchanger using a nanofluid as the working fluid. They are:

- a counter flow double pipe heat exchanger as studied by Agromayor et al. [28], and
- a single pipe heat exchanger as studied by Martínez-Cuenca et al. [29] and Mondragón et al. [30]

The double pipe heat exchanger (Agromayor et al. [28]), shown in Fig. 1, consists of the inner pipe separating both heat transfer fluids, with an inner diameter of $d_1 = 8$ mm and an outer diameter of $d_2 = 10$ mm. The outer pipe has an inner diameter of $d_3 = 15$ mm and is insulated so that heat losses to the environment can be neglected. Cold nanofluid is circulated through the inner pipe and enters the heat exchanger from the right side, while hot water circulates through the outer annulus and enters from the left side. Consequently, the nanofluid is heated by the water. The section where heat transfer occurs is 930 mm long. The pressure drop is determined with a differential pressure sensor on a 1180 mm long section. In the mathematical model, the inlet and outlet positions of the annulus were not taken into account, so the same conditions are assumed for the entire length over which the heat transfer takes place (only the average heat transfer coefficient is calculated).

The single pipe heat exchanger (Martínez-Cuenca et al. [29]) has an inner diameter d_1 of 31.2 mm, with a 3.6 mm thick wall. The test section is 1000 mm long. Cold nanofluid is circulated through the inner pipe, where it is heated by a set of band heaters. Since only the inner diameter of the pipe is relevant for single pipe heat exchangers, no geometry is presented here but can be found in the reference given above.

2.1. Fluid properties

The properties of nanofluids, such as density, thermal conductivity, heat capacity, and viscosity depend, on the temperature and concentration of the nanoparticles and are usually determined experimentally. Therefore we assume that there is a certain degree of uncertainty in these parameters. We consider the material properties as random variables and assume that the probability density function (PDF) is constant in a range around the experimentally measured data. The aim of this work is to transfer the experimentally determined uncertainty of the thermophysical properties to the desired technical results, such as the heat transfer performance of the heat exchanger.

In this work, we consider water-based nanofluids studied by Agromayor et al. [28] (graphene nanoplatelets GNP) and Mondragón et al. [30] (silica, alumina, and carbon nanotubes (CNT)). The graphene nanoplatelet (GNP) nanofluids have attracted attention mainly due to the very high thermal conductivity of graphene, i.e., $\approx$ 5000 W/m K, being around more than two orders of magnitude greater than common metal-oxide nanoparticles, and more than 50% higher than that of carbon nanotubes [31]. Agromayor et al. [28] considered nanoparticle concentrations of 0.25 wt%, 0.5 wt%, 0.75 wt% and 1 wt% in the temperature range of 15 °C to 45 °C. Mondragón et al. [30] characterised silica 1 vol% (Sil100), 5 vol% (Sil500), alumina 1 vol% (Alu100), 5 vol% (Alu500), and carbon nanotubes 0.125 vol% (CNTs012) nanofluids in the temperature range of 40 °C to 80 °C. In Fig. 2 the thermophysical properties are shown along with the reported experimental uncertainty.

We fitted for each nanofluid of a certain nanoparticle concentration a temperature-dependent function for each of the nanofluid thermophysical properties $f(T)$. The uncertainties used as inputs in the SCM method were determined at the highest experimental uncertainties of the thermophysical properties of the nanofluids in the entire temperature range. PDF for each thermophysical property was assumed constant between $(1-\omega)f(T)$ and $(1+\omega)f(T)$, where ω is the highest experimental uncertainty. In Table 1 we present the estimated uncertainty ω values and we observe that for the graphene nanoplatelets (GNP) the density has the smallest uncertainty (0.05%), while the heat capacity uncertainty is higher (about 3%). In general the highest uncertainty is observed for thermal conductivity (about 5%) and dynamic viscosity (4%). Specifically, the largest uncertainty (14%) is observed for the heat capacity of alumina 5 vol% nanofluid. The heat capacity uncertainties were estimated as the maximum difference between experimental values and those calculated with the mixture rule. Since the density of silica, alumina, and CNT nanofluids was not measured and since density has an almost negligible uncertainty, we copy the estimate of uncertainty for GNP nanofluid from Agromayor et al. [28]) and use the same value for silica, alumina, and CNT nanofluids.

2.2. Empirical estimate of heat transfer in pipe-in-pipe heat exchanger

2.2.1. Estimate of overall heat transfer coefficient

To estimate the overall heat transfer coefficient U, we assume that the heat exchanger is clean and there are no deposits on the heat

Table 1
Estimated uncertainties of fluid properties for the graphene nanoplatelets, silica, alumina, and carbon nanotubes nanofluid based on experimental results of Agromayor et al. [28] and Mondragón et al. [30]. Worst case scenario is considered, i.e., the highest experimental uncertainty is chosen from all nanoparticle concentrations and temperatures studied (Fig. 2).

	Agromayor et al. [28], GNP	Mondragón et al. [30]				
		Sil100	Sil500	Alu100	Alu500	CNTs012
Density	0.05%	0.05%	0.05%	0.05%	0.05%	0.05%
Heat capacity	3.0%	2.09%	3.61%	3.07%	14.12%	0.98%
Thermal conductivity	5.0%	3.69%	2.66%	5.84%	1.36%	1.53%
Dynamic viscosity	4.0%	2.98%	3.94%	3.18%	1.79%	3.46%

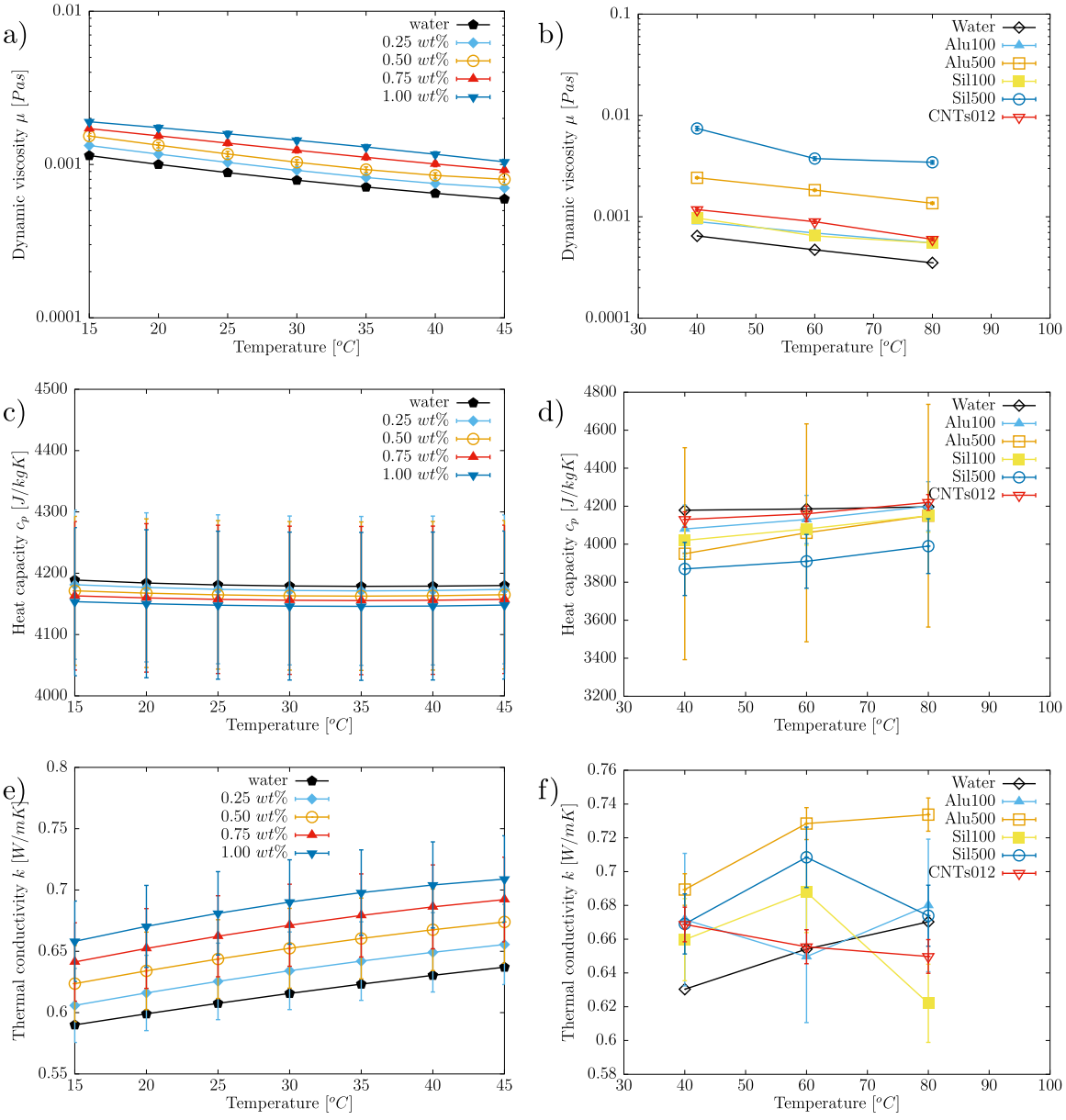

Fig. 2. Temperature dependent nanofluid properties used in the study obtained from temperature dependent models for properties. Figures (a), (b), and (c) show graphene based nanofluid used by Agromayor et al. [28] and (d), (e), and (f) show the nanofluids used by Mondragón et al. [30].

exchanger surface (no fouling). In the case of the double pipe heat exchanger, where hot water (annulus) and cold nanofluid (inner pipe) are separated by the pipe wall, the overall heat transfer from the hot to the cold fluid depends on three heat transfer mechanisms: convective heat transfer from the hot water to the outer pipe wall, conduction through the pipe wall separating both fluids, and convective heat transfer from the inner wall to the nanofluid.

Since geometrical properties of the heat exchanger are known, the total heat transfer area A is defined as on the outer area of the inner pipe separating both fluids (d_2). Overall heat transfer coefficient U (calculated for the outer wall of the inner pipe) for the heat exchanger considered here is calculated as

$$\frac{1}{U} = \frac{1}{h_w} + \frac{d_2}{2k_{wall}} \ln\left(\frac{d_2}{d_1}\right) + \frac{d_2}{h_{nf} d_1}, \qquad A = \pi d_2 L \tag{1}$$

where h_w represents convective heat transfer coefficient for the hot water (annulus), h_{nf} represents convective heat transfer coefficient for the nanofluid in the inner pipe, and k_{wall} is the thermal conductivity of the pipe material.

2.2.2. Estimate of the inner pipe heat transfer coefficient

At the nanofluid side (inner pipe) the heat transfer coefficient is calculated using two correlations. First the standard Gnielinski correlation [32], which was developed for a single phase fluid, and, second, the Agromayor et al. [28] correlation, which was derived from the experimental data using GNP nanofluid in a pipe-in-pipe heat exchanger. Both are described below.

The Reynolds (Re_{nf}) and Prandlt (Pr_{nf}) number for the nanofluid are calculated using fluid properties taken at the average temperature $T_{nf,avg}$ using the characteristic velocity obtained from the known volumetric flow rate and characteristic length d_1.

The Gnielinski correlation [32] for the heat transfer coefficient from the pipe wall to the nanofluid reads as:

$$h_{nf} = \frac{Nu_{nf} k_{nf}}{d_1}, \qquad Nu_{nf} = \frac{(\xi_{nf}/8)(Re_{nf} - 1000)Pr_{nf}}{1 + 12.7\sqrt{\xi_{nf}/8}(Pr_{nf}^{2/3} - 1)} \tag{2}$$

where friction factor ξ_{nf} is calculated from correlation for the smooth pipe, proposed by Petukhov [33]

$$\xi_{nf} = (0.79 \ln(Re_{nf}) - 1.64)^{-2}. \tag{3}$$

The second correlation that was used to estimate the Nusselt number in the inner pipe was the correlation proposed by Agromayor et al. [28], which was derived from the experimental data. The Nusselt number depends on the nanoparticle volume fraction ϕ_v

$$Nu_{nf} = 0.011(1 + 100\phi_v)^{-0.095} Re_{nf}^{0.886} Pr_{nf}^{0.545} \left(\frac{Pr_{nf}}{Pr_{nf,wall}}\right)^{-0.495} \tag{4}$$

where the factor (Pr_{nf}/Pr_{wall}) takes into account the effect of the temperature profile that depends on the heat transfer mode (if the fluid is cooled or heated). In the experiments performed by Agromayor et al. [28] the heat was transferred from the annulus (hot water) to the nanofluid, so the equation is only valid when the nanofluid is heated. The Prandtl number Pr_{wall} is calculated for the nanofluid properties at the temperature of the wall $T_{wall,nf}$ that is in contact with the nanofluid. $T_{wall,nf}$ is calculated from the total heat transfer rate from the hot water to the nanofluid and the average water temperature as

$$T_{wall,nf} = T_{w,avg} - \frac{\dot{m}_w c_{p,w}(T_{w,in} - T_{w,out})}{U_{par} A}, \tag{5}$$

where A is the outer surface area of the heat exchanger and U_{par} is the heat transfer coefficient describing heat flow from hot water and through the steel wall. Considering the resistance of heat transfer from the hot water to the inner pipe outer wall and the conduction through the pipe separating both fluids the heat transfer coefficient can be calculated as

$$\frac{1}{U_{par}} = \frac{1}{h_w} + \frac{d_2}{2k_{wall}} \ln\left(\frac{d_2}{d_1}\right). \tag{6}$$

We note that apart from the Reynolds and Prandtl numbers, Eq. (4) also includes the nanoparticle volume fraction. This indicates that Nusselt number correlations developed for single phase fluids will struggle to correctly describe the heat exchanger operating with a nanofluid. The effective medium theory assumes that all the effects related to nanoparticles are described by the effective thermophysical properties and, thus, additional terms involving particle volume fraction should not be present.

2.2.3. Estimate of the outer pipe heat transfer coefficient

Heat transfer coefficient for the hot water flowing through the annulus is calculated from correlations proposed by Gnielinski [34] and are valid for fully developed turbulent flows in annular ducts, with adiabatic outer surfaces

$$h_w = \frac{Nu_w k_w}{d_h}, \qquad Nu_w = \frac{(\xi_w/8)Re_w Pr_w}{k_1 + 12.7\sqrt{\xi_w/8}(Pr_w^{2/3} - 1)} \left[1 + \left(\frac{d_h}{L}\right)^{2/3}\right] F_w \tag{7}$$

with

$$k_1 = 1.07 + \frac{900}{Re_w} - \frac{0.63}{(1 + 10Pr_w)} \tag{8}$$

$$\xi_w = (1.8 \log_{10}(Re^*) - 1.5)^{-2} \tag{9}$$

$$Re^* = Re_w \frac{[1 + a^2]\ln a + [1 - a^2]}{[1 - a]^2 \ln(a)} \tag{10}$$

$$F_{w,in} = 0.75\ a^{(-0.17)} \tag{11}$$

where $d_h = d_3 - d_2$ is the hydraulic diameter, and ξ_w is the friction factor for the annular pipe that depends on the ratio $a = (d_2/d_3)$ (heat transfer depends on the ratio, since maximum velocity is shifted to the inner wall when a decreases). Re_w and Pr_w are using hydraulic diameter for the characteristic length. Correction factor $F_{w,in}$ is used to describe the heat transfer mode. In case of heat transfer at the inner wall, the equation of the insulated outer wall (11) is then used.

2.2.4. ϵ- NTU method for overall heat transfer rate

The effectiveness-NTU method [33] provides an estimate of the overall heat transfer rate in a pipe-in-pipe heat exchanger. The two fluids in the heat exchanger are the nanofluid (denoted by nf), entering with temperature $T_{nf,in}$ in the inner pipe, and water (denoted by w), entering with temperature $T_{w,in}$ in the outer annulus. In the first step we find the minimum heat capacity rate C_{min} (quantity of heat a fluid at certain mass flow rate is able to absorb/release per unit time) and maximum heat capacity rate C_{max} as

$$C_{min} = \min[\dot{m}_{nf} c_{p,nf}, \dot{m}_w c_{p,w}], \qquad C_{max} = \max[\dot{m}_{nf} c_{p,nf}, \dot{m}_w c_{p,w}]. \tag{12}$$

With this, the theoretical maximum possible heat transfer $\dot{Q}_{max}$ that can be achieved in a counter-flow heat exchanger of infinite heat exchange area (length) can be calculated as

$$\dot{Q}_{max} = C_{min}(T_{w,in} - T_{nf,in}). \tag{13}$$

With known maximum heat transfer rate, the effectiveness $\epsilon = \dot{Q}/\dot{Q}_{max}$ of the heat exchanger is calculated as the ratio between actual heat transfer rate $\dot{Q}$ and maximum possible heat transfer rate. The value of ϵ is in the range between 0 and 1, where 1 represents perfect exchange. For a double pipe heat exchanger with counter-flow arrangement, the effectiveness ϵ may also be estimated [33] as

$$\epsilon = \frac{1 - \exp[-NTU(1 - C_r)]}{1 - C_r \exp[-NTU(1 - C_r)]} \tag{14}$$

where $C_r = C_{min}/C_{max}$ is the heat capacity rate ratio, and $NTU = \frac{UA}{C_{min}}$ is the number of transfer units. Since outlet temperatures are unknown, the heat transfer rate is estimated by

$$\dot{Q} = \epsilon C_{min}(T_{w,in} - T_{nf,in}). \tag{15}$$

With known heat transfer rate from one fluid to another, outlet temperatures for each pipe are calculated using the energy balance equation

$$T_{nf,out} = T_{nf,in} + \frac{\dot{Q}}{c_{p,nf}\dot{m}_{nf}}, \qquad T_{w,out} = T_{w,in} + \frac{\dot{Q}}{c_{p,w}\dot{m}_w}. \tag{16}$$

2.2.5. Pressure drop through the inner pipe

Pressure drop through the inner pipe, needed to evaluate some figure of merits (FOMs), is calculated using the Darcy–Weisbach equation

$$\Delta p_{nf} = \xi_{nf} L_{\Delta p} \frac{\rho u_{nf}^2}{2d_1} \tag{17}$$

where the friction factor ξ_{nf} is depends on which correlation is used to calculate the Nusselt number. For the case where the Gnielinski correlation [32] is used, the friction factor is calculated from $\xi_{nf} = (0.79\ln(Re_{nf}) - 1.64)^{-2}$, and for the case where correlations proposed by [28] are used, the following correlation is used

$$\xi_{nf} = 0.109(1 + 100\phi_v)^{0.215} Re_{nf}^{-0.159}. \tag{18}$$

2.2.6. Algorithm

The task described above, evaluating the performance of a double pipe heat exchanger, is non-linear because the fluid properties depend on the local fluid temperature, which is unknown within the heat exchanger. Therefore, an iterative approach is taken to obtain the solution. Starting from an initial estimate for the fluid temperature, we iterate until convergence is reached. The fluid properties are evaluated at the average temperature between inlet and outlet temperature. The outlet temperature in the numerical model is unknown and is estimated during the iterative procedure.

The inlet temperatures are known for all considered cases and are set as follows: the inlet temperature of the nanofluid is set to $T_{nf,in} = 28.5$ °C and of the hot water to $T_{w,in} = 40.9$ °C. The volumetric flow rate of the hot water is constant, equal to 800 l/h, and the flow rate of the nanofluid ranges from 200 to 700 l/h with 100 l/h steps.

The following algorithm is used to estimate the heat transfer in a double pipe heat exchanger.

1. Initial guess of the outlet temperature of both heat transfer fluids is the arithmetic mean of both inlet temperatures: $T_{nf,out} = T_{ann,out} = (T_{nf,in} + T_{nf,in})/2$.
2. Iterative loop.
   (a) Calculate the average temperature of each fluid ($T_{nf,avg}, T_{ann,avg}$) at which the fluid properties are evaluated.
   (b) Calculate the heat transfer coefficient for each pipe, Eqs. (2) and (7).
   (c) Calculate the overall heat transfer coefficient U using Eq. (1).
   (d) ϵ- NTU method: obtain the overall heat transfer rate $\dot{Q}$ (Eq. (15)) and new outlet temperature of each fluid (Eq. (16)).
   (e) If the convergence criteria $abs(T_{avg}^{new} - T_{avg}^{old}) \leq 0.01\ K$ is reached, finish the inner loop and go to 3. If not, repeat the loop (T_{avg}^{new} is the new average temperature of each fluid and T_{avg}^{old} is the average temperature at which fluid properties were evaluated).
3. Evaluate final estimates for relevant quantities $T_{nf,out}$, Re_{nf}, Pr_{nf}, Nu_{nf}, h_{nf}, h_w, Δp_{nf}, $LMTD$, U, $\dot{Q}$.
4. Evaluate the FOM expressions.
5. End the calculation.

2.3. Empirical estimate of heat transfer in a single pipe heat exchanger

For a single pipe heat exchanger, the temperature at which the fluid properties are estimated is the inlet temperature of the nanofluid. Since, in this case, a single pipe heat exchanger is used, no iteration loop is needed. For the case of heat transfer in a single pipe heat exchanger with constant heat flux, the heat transfer coefficient for the nanofluid is calculated from the Gnielinski correlation (2). The pressure drop through the pipe is calculated from Eq. (17), where the length of the pipe (1000 mm) and friction factor obtained from (3) are used for the calculation.

2.4. Figures of merit

In nanofluid literature, figures of merit (FOMs) have been frequently used. FOMs provide direct, mostly thermophysical property-based and system type-based performance assessments of heat transfer fluids. Specifically, FOMs have been used to assess nanofluid cooling performance [35–37], as well as in circular jet impingement [38], forced circulation loops [39], under laminar flow [40], and under both laminar and turbulent flow [41] conditions. Detailed descriptions of FOMs can be found in the literature (for example, in [37,42,43]). Here, the most commonly used FOM descriptions are provided.

When a thermal performance comparison is to be performed, it is common to compare the heat transfer coefficients of the nanofluid and its base fluid. For ratios larger than one, use of the considered nanofluid could be regarded as advantageous.

On the other hand, the necessity of accounting for as much of the expenses as possible has become as critical as accounting for the improvements. The definition of performance and thus FOMs in this regard should also cover expenses such as increased pumping power requirements. Considering the hydrodynamic nature of the nanofluid flow along with the thermal features (the latter usually being more advantageous than those of the base fluids) provides a more realistic picture.

The Mouromtseff number (Mo) is among the most commonly used FOMs in the literature, and defined dependent on the working fluid density, thermal conductivity, specific heat capacity, and viscosity; thereby providing a comprehensive overview of the utility of the working fluid, both from thermal and hydrodynamic behaviour points of view.

Having a Nusselt number correlation for a specific heat transfer device in mind [42], the Mouromtseff number can be derived by expressing the heat transfer coefficient and grouping all material properties into the Mouromtseff number:

$$Nu = f(Re, Pr, \mathcal{L}), \qquad \Rightarrow \qquad h = \underbrace{\left(\frac{\rho^a k^b c_p^d}{\mu^e}\right)}_{Mo} f'(u, \mathcal{L}) \tag{19}$$

where $\mathcal{L}$ is the characteristic dimension of the heat transfer device and u is the flow velocity. For example, for internal turbulent flow, the exponents are reported as $a = 0.8$, $b = 0.67$, $d = 0.33$, and $e = 0.47$ by [44]. The significance of the Mouromtseff number lies in the fact that, for flow over or through a given geometry at a specified velocity, the heat transfer fluid with the largest Mouromtseff number will provide the highest heat transfer rate.

As nanofluids have been introduced to the agendas of both heat transfer research and industry, the importance of FOMs has increased, as they provide a direct, qualitative, and quantitative result in terms of the nanofluid being more advantageous or not in comparison to its base fluid counterpart. Since Mo is a dimensional number, Mo ratio (Mo_r) has been used instead [37] as a FOM. For the case of comparing the performance of a nanofluid and water in a given heat exchanger at a chosen flow velocity, Mo_r can be calculated as the ratio of heat transfer coefficients:

$$Mo_r = \frac{h_{nf}}{h_w} \tag{20}$$

If $Mo_r > 1$, the nanofluid will be more effective in transporting heat than water.

One other FOM is the PEC ratio, i.e., PEC_r, providing another comprehensive comparison considering both the heat transfer and hydrodynamic behaviour, as in Eq. (21), which is applicable for both laminar and turbulent flow conditions

$$PEC = \frac{\dot{m} c_p \Delta T}{\dot{V} \Delta p}, \qquad \Rightarrow \qquad PEC_r = \frac{PEC_{nf}}{PEC_w}. \tag{21}$$

Using nanofluid is beneficial when $PEC_r > 1$.

Although their use was observed less frequently in the literature, the Overall Energetic Efficiency (η) [45] and Energy Ratio (ER) [46] are two other comprehensive FOMs, are defined in Eqs. (22) and (23), respectively:

$$\eta = \frac{Nu_{nf}}{Nu_w} \cdot \frac{\xi_w}{\xi_{nf}} \tag{22}$$

$$ER = \frac{Nu}{Eu}, \qquad Nu = \frac{hd_1}{k}, \qquad Eu = \frac{\Delta p}{\rho u^2} \tag{23}$$

In Eq. (23) u is the fluid mean velocity in the inner pipe. The ER provides a thermal-hydrodynamic flow characteristic comparison, which takes into account the advantages of high heat transfer coefficient (high Nu) and disadvantages of viscous losses with nanofluids (high Eu). For fully developed internal laminar flow, Nu approaches a constant value, making η (Eq. (22)) and ER (Eq. (23)) based completely on pressure drop ratios and hydrodynamic character of the flow, respectively, thereby somewhat eliminating the thermal character in both FOMs.

The final FOM considered in this paper is the thermal performance factor η_{tf}, defined as [47]:

$$\eta_{tf} = \frac{Nu_{nf}}{Nu_w} \left(\frac{\xi_w}{\xi_{nf}} \right)^{1/3} \tag{24}$$

In Eqs. (22) and (24), the Nusselt number Nu_w is calculated by considering that pure water is flowing in the inner pipe instead of the nanofluid.

2.5. Stochastic collocation method

We consider nanofluid properties σ_i such as thermal conductivity, density, heat capacity and nanoparticle concentration to be random variables uniformly distributed in a range $\sigma_i \in (\sigma_{i,min}, \sigma_{i,max})$. Their probability distribution function (PDF) is

$$P(\sigma) = \begin{cases} \frac{1}{\sigma_{max} - \sigma_{min}} & \sigma \in (\sigma_{min}, \sigma_{max}) \\ 0 & elsewhere \end{cases} \tag{25}$$

Let the number of random variables be n. Additionally, let us designate the empirical calculation of heat exchanger heat transfer efficiency, described in the previous sections, as $y(\sigma_1, \ldots, \sigma_n)$. To calculate the expected value μ_y and variance var_y of the deterministic model, we use:

$$Y_i = \int_{-\infty}^{\infty} \ldots \int_{-\infty}^{\infty} \left[y(\sigma_1, \ldots, \sigma_n) \right]^i P(\sigma_1) \ldots P(\sigma_n) d\sigma_1 \ldots d\sigma_n \tag{26}$$

$$\mu_y = Y_1, \qquad var_y = Y_2 - \mu_y^2 \tag{27}$$

We calculate the integral (26) numerically, using the Smolyak [48,49] sparse grid approach. The integral is approximated by

$$Y_i \approx \sum_{i=1}^{N} \left[y\left(\sigma_{1,i}, \sigma_{2,i}, \ldots, \sigma_{n,i}\right) \right]^i w_i, \tag{28}$$

where η_i and w_i are sparse grid points and weights. The deterministic model has to be evaluated N times, once for each of the selections of random variables (nanofluid parameters). The accuracy of numerical integration depends on the number of realisations of the deterministic model N. This value may be increased as necessary and, due to the sparse approach, is much smaller than the number that would be needed by a full grid approach, such as a Gauss Legendre quadrature. Additional details of the implementation of the Stochastic Collocation Method are given by Šušnjara et al. [50].

2.6. Statistical assessment

Even though nanofluids are characterised by high thermal conductivity, the assessment of a heat transfer fluid's applicability in a convective transfer setting depends highly on the viscosity, pressure drop, and pumping power requirement, as well as factors affecting them [51]. Other than stationary settings, viscosity is as important as the thermal conductivity for heat transfer with nanofluids [31]. One of the main issues with nanofluids has long been the optimisation of the enhanced thermal performance and increased pressure drop caused by enhanced nanoparticle loading in forced convective heat transfer applications. Hence, it is important to consider the full system and multiple practical variables in a realistic manner in order to uncover the thermal and hydrodynamic behaviours of nanofluids simultaneously.

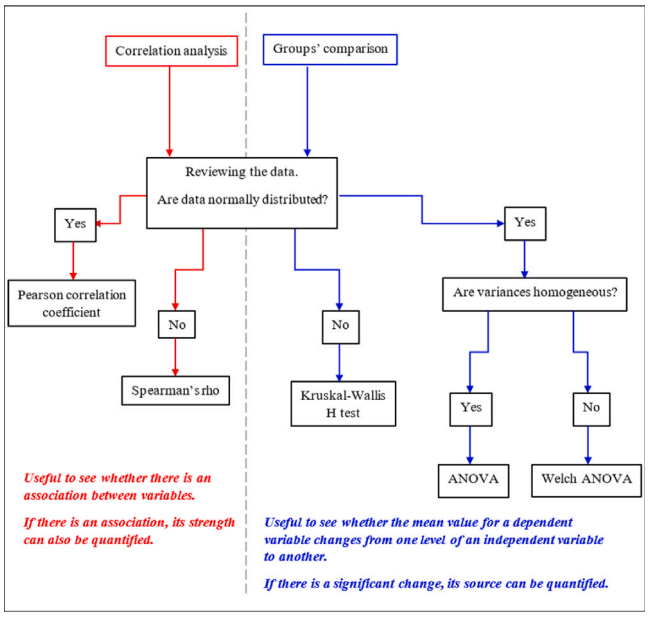

Fig. 3. Methodology followed in statistical assessment.

To assess the metal-oxide and graphene nanoplatelet nanofluid heat transfer and hydrodynamic performances in a combined way, we process the heat transfer coefficient and pressure drop values reported by [28,29], which are experimental results. We also process the data as the outcome of the numerical experiments simulated in this current work, using the Gnielinski correlation (and for GNP nanofluids data, the correlations proposed by [28]), to shed light on how experimental as well as numerical approaches capture heat transfer coefficient — pressure drop relationship of the wide range of nanofluids studied. For this purpose, in Part 1 (Section 3.5), we report on the results of correlation analyses on heat transfer coefficient and pressure drop values for the studied nanofluids data. These are considered as direct indicators of performance. In Part 2 (Section 3.6), we report on the experimental Nu and friction factor data by [28,29], more as performance-related (yet, indirect) variables and, hence, decision-making tools for nanofluid based convective heat transfer systems. The rigorous statistical methodology followed in this work is provided as a flowchart in Fig. 3.

3. Results

3.1. Numerical integration accuracy analysis

We performed a sparse grid numerical integration accuracy analysis by repeating a single case with four different sparse grid setups with 3 collocation points (CP) (81 realisations of the deterministic model), 5 (625 realisations), 7 (2401 realisations), and 9 collocation points (6561 realisations). We used the case $\phi_v = 0.5\%$ and $\dot{V} = 400\ l/h$ and analysed the difference in expected value and variance. Comparing the results for 3 and 9 collocation points, we observe an average relative difference (3CP-9CP)/9CP in the expected value of $1.5 \cdot 10^{-3}$ and in the variance of $7.4 \cdot 10^{-3}$. Comparing the results of 7CP and 9CP, we find

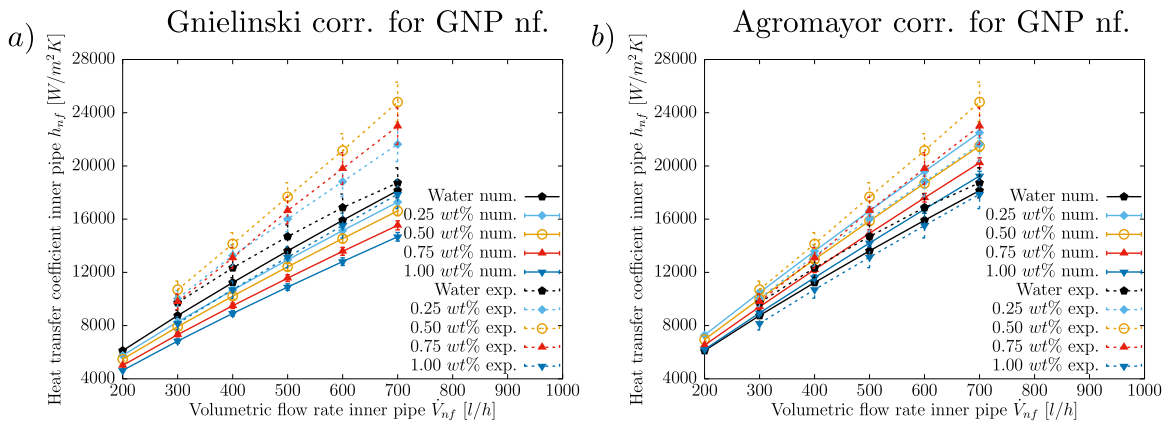

Fig. 4. Expected values and standard deviations of inner pipe heat transfer coefficient in the pipe-in-pipe heat exchanger using GNP nanofluid. Panel (*a*) Gnielinski [32] and (*b*) Agromayor et al. [28] correlations.

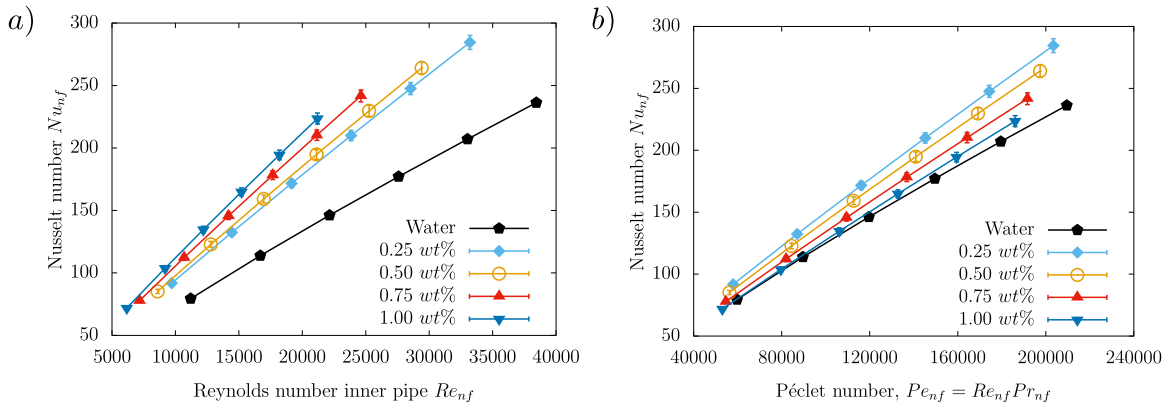

Fig. 5. Expected values and standard deviations of inner pipe Nusselt number in the pipe-in-pipe heat exchanger using GNP nanofluid obtained using Agromayor et al. [28] correlation. Panel (*a*) shows the dependence versus the Reynolds number, panel (*b*) versus the Péclet number.

that the average relative difference for the expected value is $3.5 \cdot 10^{-5}$ and for the variance $3.5 \cdot 10^{-4}$. This proves a good convergence of the numerical integration. For the analytical part of the calculation (Nusselt number estimates), we used 7 collocation points (2401 realisations) in the further analysis.

3.2. Pipe-in-pipe heat exchanger

We analysed the pipe-in-pipe heat exchanger twice, first with the Gnielinski correlation [32] and then with the correlation of Agromayor et al. [28]. The Gnielinski correlation is used in the standard procedure available to engineers to estimate heat transfer coefficients in fully developed turbulent flow regimes in tubular heat exchangers. The correlation of Agromayor et al. [28] was developed specifically for the selected GNP nanofluid in the pipe-in-pipe heat exchanger. Looking at the comparison between the estimated heat transfer coefficient in the inner pipe h_{nf} and the measured values (Fig. 4), we find that the correlation of Agromayor et al. [28] shows much better agreement with the experimental data. This is to be expected as the correlation was tailored to the GNP nanofluid and the pipe-in-pipe heat exchanger.

In Fig. 5 we show the expected value of the inner pipe Nusselt number in the pipe-in-pipe heat exchanger using GNP nanofluid obtained using Agromayor et al. [28] correlation. We can see that the standard deviation is smaller than the change of the Nusselt number due the change in nanoparticle concentration. Comparison of the relationship with Reynolds number (Fig. 5a) and Péclet number (Fig. 5b) shows an increase in Nusselt number with nanoparticle concentration for a fixed Reynolds number. As the nanoparticle concentration increases, the heat diffusivity increases, which leads to improved heat transfer at fixed flow regime. On the other hand, the increase in heat diffusivity leads to a smaller Péclet number for a given flow rate. So we see that for a fixed ratio between convective and diffusive heat transfer (i.e. for a fixed Péclet number), the Nusselt number decreases with increasing nanoparticle concentration.

The Gnielinski correlation [32] significantly underestimates the heat transfer coefficient for all flow rates and gives values that are even lower than when using pure water in the inner pipe. This indicates that the GNP nanofluid exhibits a behaviour that is significantly different from that of a standard Newtonian fluid. When we compare the uncertainties in the heat transfer coefficient, we find that they are of the same order of magnitude for both correlations. In the case of Agromayor et al. [28], the difference between the experimentally determined and the SCM expected value of the heat transfer coefficient is within the uncertainty limits. For the Gnielinski correlation [32] this is not the case. This underlines the conclusion that the uncertainty in the performance of heat exchangers with GNP nanofluid cannot be attributed only to the uncertainty in the properties of the nanofluid and, therefore, the standard empirical correlation should not be used. This is confirmed by Calvino et al. [52], who stated that the turbulent mixing phenomenon within the nanometric dispersion provides a superior benefit in terms of the heat transfer performance than the modified intrinsic transport property of the two-phase sample. Graphene nanoplatelets act as nanoobjects and not as nanoparticles, whose effect could be completely described by effective transport properties. Another significant difference between the model and the experiment is that the best heat transfer fluid according to the model is the one with a GNP mass concentration of 0.25 wt% and not 0.5 wt% as found in the experiment.

Table 2
Difference between the SCM determined expected value and experimentally [28] determined value of the heat transfer coefficient expressed as percent error. Expected values were obtained using the Gnielinski and Agromayor et al. [28] correlations in the pipe-in-pipe heat exchanger. The green italic font denotes that the expected value with its confidence interval is inside the confidence interval of the experimental measurement.

ø	Water	0.25 wt%		0.50 wt%		0.75 wt%		1.00 wt%	
$\dot{V}$ [l/h]	Gni.	Gni.	Agr.	Gni.	Agr.	Gni.	Agr.	Gni.	Agr.
300	−10.0%	−17.4%	*4.5%*	−26.0%	*−6.5%*	−25.2%	*−3.9%*	−16.2%	9.6%
400	−8.9%	−19.6%	*2.5%*	−27.7%	−8.2%	−27.5%	*−6.7%*	−16.7%	8.4%
500	−7.3%	−19.2%	*3.8%*	−29.8%	−10.3%	−30.5%	−10.3%	−17.1%	8.1%
600	*−5.7%*	−19.6%	*4.1%*	−31.2%	−11.6%	−31.4%	−11.1%	−17.4%	*7.9%*
700	*−3.1%*	−20.1%	*4.1%*	−33.0%	−13.4%	−32.4%	−12.0%	−17.9%	*7.7%*

In Table 2, the difference between the SCM determined expected value and experimentally [28] determined value of the heat transfer coefficient expressed as percent error is shown. As can be observed, the maximum percent error between the experimental heat transfer coefficient data and the SCM expected values is −13.4%, with the majority of cases below 10%. It can also be seen that, for the GNP mass concentration 0.5 wt% and 0.75 wt%, the correlations underestimate the heat transfer coefficients, while they are overestimated for 0.25 wt% and 1.0 wt%. However, the Gnielinski correlation [32] underestimates the heat transfer coefficients for all cases to a significantly larger extent compared with the Agromayor et al. [28] correlation, with a maximum percent error of −33.0%.

The experiments were performed at fixed flow rates. Since viscosity increases with increasing concentration of nanoparticles, the Reynolds number of the nanofluid is smaller than the Reynolds number of water at the same flow rate. On the other hand, when considering a single Reynolds number, the volumetric flow rate of water is lower compared to nanofluids with increasing concentration of nanoparticles. In Fig. 6 we show the results for the average temperature and friction factor in the pipe filled with nanofluid versus the Reynolds number. We find that the average temperature decreases with the volume fraction of nanoparticles for a given Reynolds number. The increase in heat flow rate due to improved nanofluid thermophysical properties is not high enough to heat a larger volume of working fluid to the same average temperature as for the pure water case. We also find that the average temperature in the inner pipe decreases with Reynolds number. This is due to the increased mass flow rate (higher volumetric flow rates) and the increase in heat flow rate not being sufficient enough to heat larger amounts of mass (due to the increased convective heat transfer of the nanofluid h_{nf}).

The uncertainty in the average nanofluid temperature is largest at low Reynolds numbers and smallest at high Reynolds numbers. The reason for this is that convection dominates heat transfer at high Reynolds numbers and the properties of the nanofluid, such as thermal conductivity, play a less important role.

When we compare the results for the friction factor ξ_{nf} in Fig. 6b_1, where the Gnielinski correlation for the smooth pipe was used (3), to the experimental correlation proposed by Agromayor et al. (18) in Fig. 6b_2, we can observe that the friction factor obtained from the Gnielinski correlation is higher than that of the correlation based on the experimental data. Experimental data reveal that the friction factor also depends on nanoparticle volume concentration. This phenomena cannot be captured by the pure fluid correlation for the smooth pipe (9) since friction factor for the smooth pipe case depends only on the Reynolds number. However, the justification for using this correlation is that the obtained results for the heat transfer coefficient of the pure water is in good agreement with the experiment (Fig. 4). Consequently, due to the fact that we are using the assumption that the nanofluid can be completely described by effective thermophysical properties, the friction factor should stay the same. This, as we can observe from the numerical data, is not the case. Since SCM estimates small uncertainty for the friction factor, the reason for the discrepancy is not the uncertainty in thermophysical properties but rather with the assumption that the nanofluid can be completely described by effective thermophysical properties.

In Fig. 7a we present the LMTD results. We observe that a higher concentration of GNP nanoparticles leads to an increase in LMTD. This is expected since, due to the lower heat transfer coefficient, the average nanofluid temperature decreases, leading to an increase in LMTD with an increase in the GNP nanoparticle concentration. Due to the constant inlet temperatures, the outlet temperature for each working fluid depends on the heat transfer coefficient. Consequently, the LMTD calculated from the inlet and outlet temperatures is not constant. As the increase of Reynolds number enhances convective heat transfer, the higher mass flow of the nanofluid reduces the average temperature of the nanofluid (temperature difference between nanofluid inlet and outlet temperature) and, hence, we observe a decrease in LMTD.

In the case where we have a GNP concentration of 0.25 wt% the Agromayor et al. [28] correlation predicts an LMTD similar to that of the pure water case (Fig. 7a_2). This is due to the fact that, in this case, the increase in the total heat transfer coefficient is lower than in cases with a higher GNP concentration.

Figs. 8 and 9 compare the Mouromtseff ratio, overall energetic efficiency, energy ratio, and PEC. The Gnielinski correlation predicts the Mouromtseff ratio and the overall energetic efficiency to be less than unity, while the Agromayor et al. [28] correlation reveals values above one. The uncertainty in figures of merit is significant, but not large enough to explain the difference between the Gnielinski correlation and the experimentally determined correlation. This supports the claim that the behaviour of the GNP nanofluid cannot be adequately described by only considering effective thermophysical properties.

The energy ratio (Nusselt over Euler number, Fig. 9a) increases with nanoparticle concentration at a chosen Reynolds number and also increases with Reynolds number at a chosen nanoparticle concentration. This indicates that the heat transfer increases faster than the frictional losses as the nanoparticle concentration and Reynolds number increase. We can conclude that heat exchanger designs operating at higher Reynolds number and at higher nanoparticle concentration have better energy ratios. This finding is also valid for the case of a single pipe heat exchanger (Fig. 11d).

The PEC_r comparing the heat flow rate and pumping power (Fig. 9b) between the use of pure water and nanofluid shows a slight dependence on the Reynolds number and increases with decreasing volume fraction of nanoparticles. The Agromayor correlations reveals PEC_r values above one, and the Gnielinski correlation yields values below one. Since using a nanofluid is beneficial as compared to using pure water at $PEC_r > 1$, the results again prove that using the Gnielinski correlation for nanofluids leads to misleading conclusions.

3.3. Single pipe heat exchanger

SCM provides expected values and variances for a number of technical parameters and FOM expressions. Panel Fig. 10a shows the comparison between the Nusselt number obtained with SCM and with experiment [29] by displaying the expected values and standard deviation. We see that for lower Re numbers, numerical results show good agreement with the experimental data. For the metal-oxide nanofluids with lower nanoparticle volume concentration (Sil100 and Alu100) the numerical data show good agreement with the experimental results over the whole Reynolds number range. However, this is not true for the nanofluids with higher nanoparticle volume concentration and carbon nanotubes (Sil500, Alu500, and CNTs012). From the experimental data, we observe that, for the Sil500 and Alu500 at $Re \approx 20000$, the heat transfer coefficient does not continue to increase as steeply, which is not the case for the model results. The same is observed for the CNT above $Re \approx 40000$. This is due to the fact that

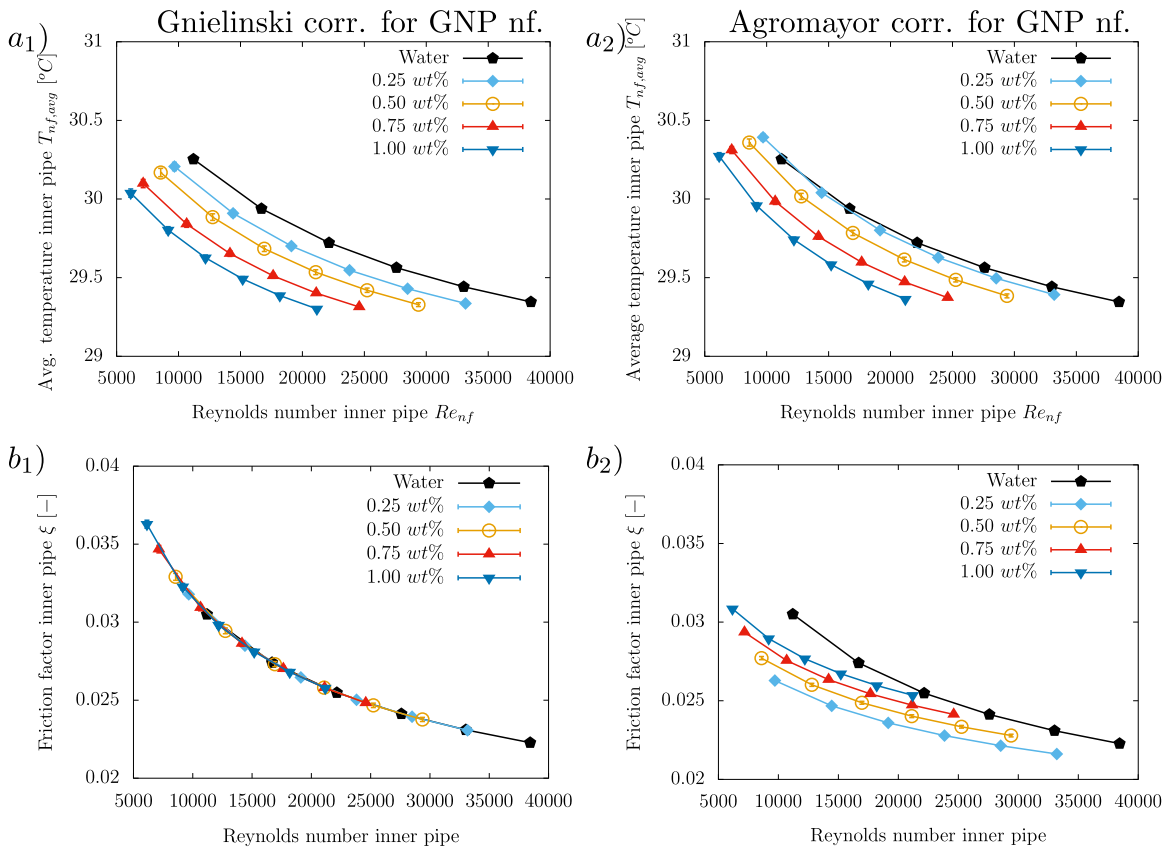

Fig. 6. Expected values and standard deviations for the pipe-in-pipe heat exchanger with GNP nanofluid. Panels (*a*) show average temperature in inner pipe and panels (*b*) show the friction factor in inner pipe obtained using the Gnilelinski [32] and Agromayor et al. [28] correlations.

convection is the dominant transport mechanism at large Reynolds numbers. For convective transport, thermophysical properties are less important than in diffusion dominated flows. It is evident that the model developed for Newtonian fluids is unable to fully capture the behaviour of nanofluids. This is in accordance with the findings of Tschisgale and Kempe [53], who discovered that nanoparticles suppress the wall-mounted turbulent structures. Changes in turbulence close to the wall affects the heat transfer mechanisms and thus models for single phase fluids are inadequate. We find that the Nusselt number increases with the concentration of nanoparticles. It shows a weaker dependence on concentration than the heat transfer coefficient, since it is defined as the ratio between heat transfer coefficient and thermal conductivity, both of which increase with the concentration of the nanoparticles. If we compare the friction factor ξ_{nf} (Fig. 10b), the numerical friction factor calculated from Eq. (3) is lower than the friction factors calculated from the experimental data. For the numerical estimation of the friction factor, the correlation for a smooth pipe was used, because the heat exchanger pipe was made of aluminium (absolute roughness 0.001–0.002 mm, relative pipe roughness $\epsilon/d_h = 3.2\text{–}6.4 \cdot 10^{-3}$). In Fig. 10b we observe that the numerical friction factor is lower than the experimental friction factor.

Plots in Fig. 10c and d show the Nusselt number and the heat transfer coefficient as a function of the Péclet number. For a fixed Péclet number, where the ratio between convective and diffusive heat transfer is fixed, we find that an increase in nanoparticle concentration leads to a decrease in heat transfer. This is to be expected because a higher nanoparticle concentration leads to a higher heat diffusivity and an increase in diffusive heat transfer, which is less efficient than convective heat transfer.

The figures of merit are presented in Fig. 11. The Mouromtseff ratio, the overall energetic efficiency, and the thermal performance factor show similar results and increase slightly with the Reynolds number. For a chosen Reynolds number, none of the FOM values are above one. The FOM uncertainty is largest in the case of the alumina nanofluid but at the same time is in all cases so small that it does not allow any alternative interpretation of the results. The energy ratio shown in Fig. 11d represents the ratio between the Nusselt and Euler numbers. Its relation to the Reynolds number is linear in all cases. The uncertainty determined by the SCM is small, which means that the uncertainty in the thermophysical properties of the nanofluid does not significantly affect the energy ratio.

3.4. Sensitivity analysis of variance

We chose to consider $n = 4$ random variables to study uncertainty propagation and carried out the analysis by considering uncertainty in all four parameters: thermal conductivity, density, heat capacity, and viscosity. Such an approach is called a Full Tensor Product (FTP) approach. Alternatively, when only one of the parameters is varied, we have the One-At-a-Time (OAT) approach. Statistical quantities may be compared between the OAT and the FTP approaches. In this way, we can study how the uncertainty of the output of the model can be apportioned to different sources of uncertainty [54]. We define the sensitivity index of each random variable as

$$S_i = \frac{var_{y,OAT(i)}}{var_{y,FTP}} \tag{29}$$

where $var_{y,OAT(i)}$ is the variance obtained using the OAT approach, with i denoting the parameter which was assumed to be a random variable. Large values of the sensitivity index indicate bigger relative importance of the random variable. We examined the case of double pipe heat exchanger with 0.5 wt% nanofluid.

The results are shown in Fig. 12, where we can observe that the nanofluid density has a very small sensitivity index. This means that

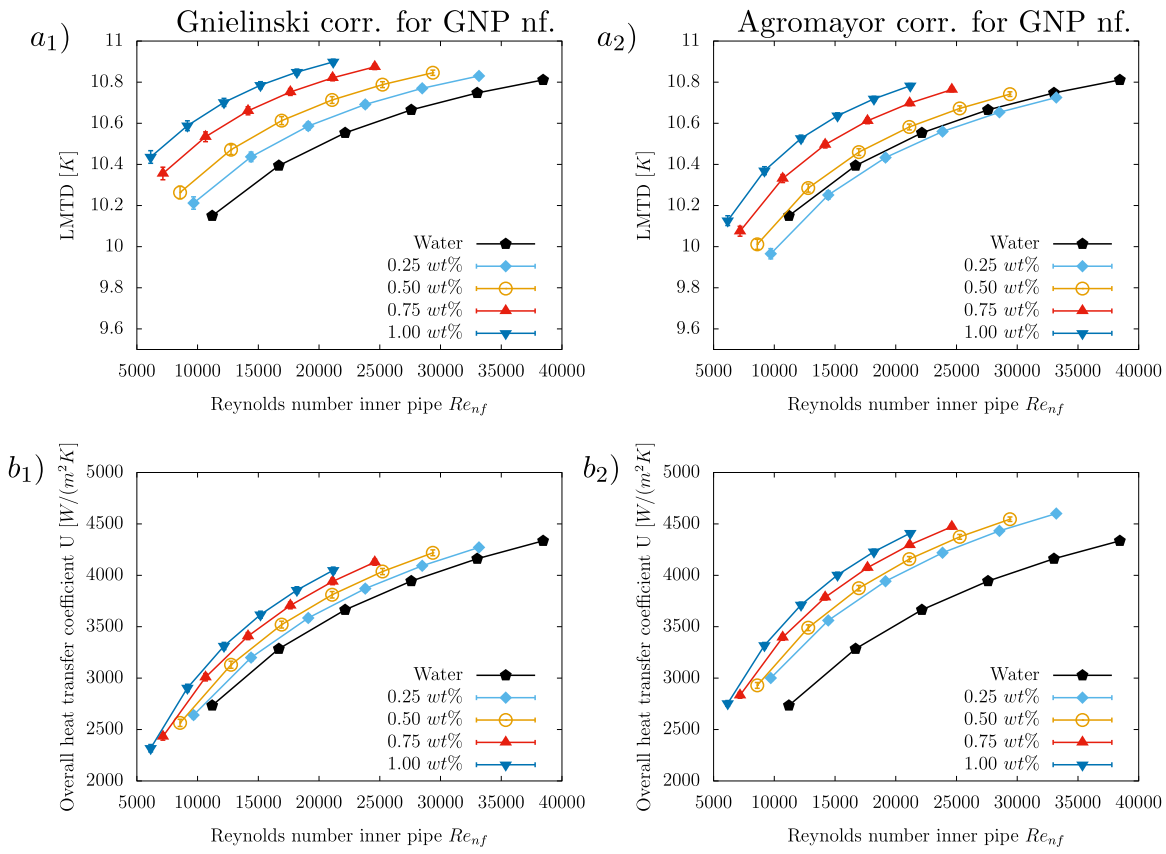

Fig. 7. Expected values and standard deviations for the pipe-in-pipe heat exchanger with GNP nanofluid. Panels (*a*) show LMTD and panels (*b*) show the overall heat transfer coefficient obtained using the Gnielinski [32] and Agromayor et al. [28] correlations.

the heat exchanger parameters such as the Nusselt number, the heat transfer coefficient, and LMTD are not influenced by the uncertainty in density measurement. In future studies, density can be omitted from the list of random variables considered and thus the total number of simulations needed to perform SCM for a nanofluid in an engineering device can be significantly reduced. This is especially important for studies which would involve more demanding mathematical models of the device, such as CFD, as reduced computational time would enable employment of more complex and accurate models.

According to Fig. 12a and b, the nanofluid thermal conductivity is the most important parameter influencing the Nusselt number and the heat transfer coefficient, while the nanofluid heat capacity has significantly less of an effect. Viscosity plays an even smaller role. On the other hand, when considering the pressure drop and friction factor, viscosity is the only influencing parameter. The LMTD is significantly influenced by the thermal conductivity and heat capacity, where the influence of the heat capacity becomes more prominent with increasing flow rate. At a constant mass flow rate, the overall heat flow rate is equally influenced by thermal conductivity and heat capacity, while the viscosity and density have a negligible effect.

3.5. Statistical assessment, Part 1: Direct indicators of the nanofluids' heat transfer performance

In this part, we are interested in how the pressure drop and heat transfer coefficient are associated for the metal-oxide and carbon nanotube [29], as well as GNP [28] nanofluids. For convenience, we refer to the analyses on the metal-oxide and carbon nanotube nanofluids as Case-1, and the analyses of the GNP nanofluids as Case-2. We further distinguish the experimental dataset (i.e., data from [28,29]) with the letter E, resulting in Case-1E and Case-2E; while for the analyses based on the numerical simulations we use the letter N, resulting in Case-1N and Case-2N.

Table 3
Correlation analyses of heat transfer coefficient and pressure drop for the metal-oxide and CNT nanofluids.

Nanofluid	ρ, Case-1E	ρ, Case-1N
Alu100	0.985	0.984
Alu500	0.948	0.985
CNTs012	0.954	0.985
Sil100	0.976	0.984
Sil500	0.886	0.986

Correlation analyses gauge the association between two variables. During correlation analyses, the following hypotheses are tested: H_0: The correlation coefficient (ρ) between variables is zero. H_a: The correlation coefficient (ρ) between variables is nonzero. After the correlation analysis is performed, we will check two output values: (i) significance value (p-value) and (ii) correlation coefficient. Based on the p-value, either H_0 or H_a is accepted. If $p > 0.05$, H_0 is accepted. Otherwise, H_a is accepted. For cases where $p \leq 0.05$, the value of the correlation coefficient (ρ) should also be interpreted. Gerber and Finn [55] expressed the extent of correlations based on $|\rho|$ ranges as follows: weak correlation for 0–0.30, moderate correlation for 0.31–0.60, and strong correlation for >0.60. Table 3 summarises the correlation coefficients between the heat transfer coefficients and pressure drops for Case-1.

The results in Table 3 show that the level of association between the heat transfer coefficient and pressure drops, as shown by the correlation coefficients computed based on the experimental data (Case-1E) and numerical data (Case-1N) being close to each other for low concentrations (see Sil100 and especially Alu100). It is further seen that, for high concentrations and/or nonspherical nanoparticle shapes, the

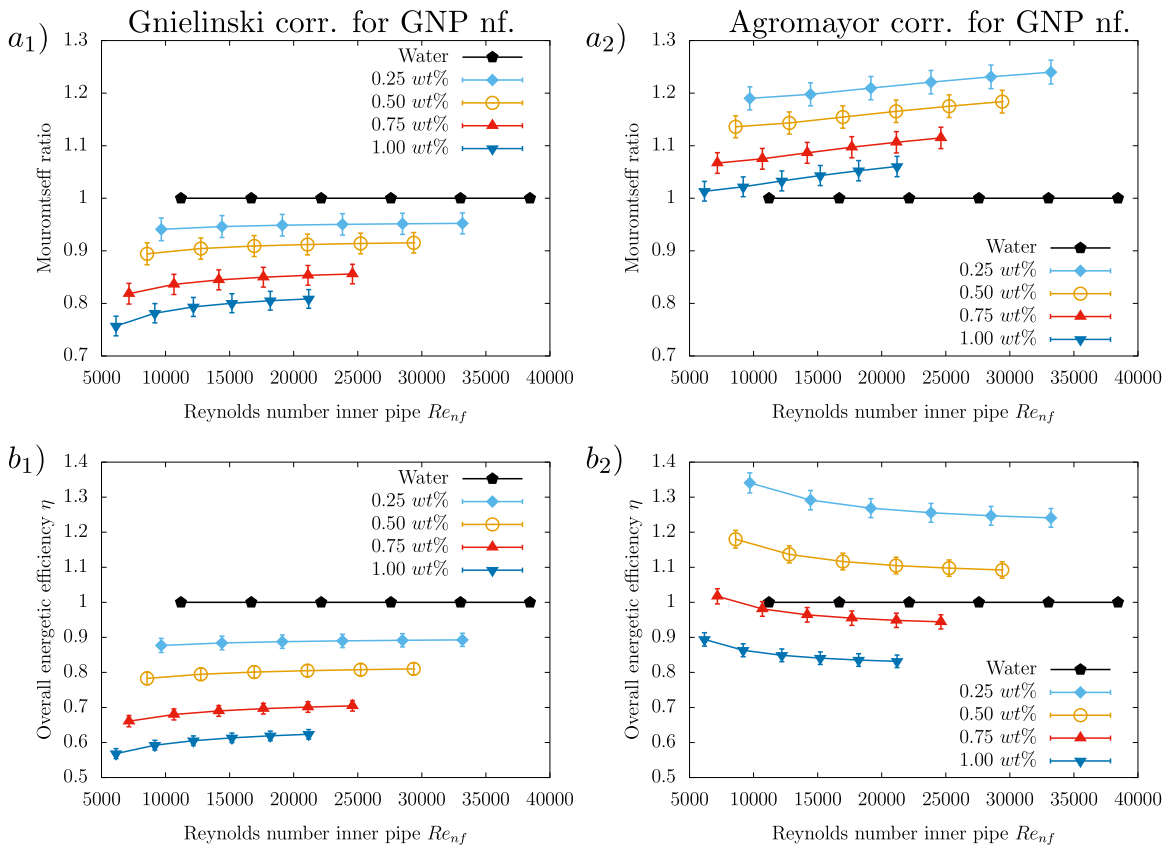

Fig. 8. Expected values and standard deviation of the Mouromtseff ratio (panels *a*) and the overall energetic efficiency (panels *b*) obtained using the Gnielinski [32] correlation and the Agromayor et al. [28] correlation. GNP nanofluid is considered in a pipe-in-pipe heat exchanger.

Table 4
Correlation analyses of heat transfer coefficient and pressure drop for the GNP nanofluids.

GNP nanofluid	ρ, Case-2E	ρ, Case-2N*	ρ, Case-2N**
0.25 wt%	0.993	0.994	0.994
0.5 wt%	0.996	0.994	0.994
0.75 wt%	0.993	0.994	0.994
1 wt%	0.994	0.994	0.994

*Gnielinski correlation [32].
**Agromayor correlation.

experimental and numerical trends tend to differ, as the extent of association between the pressure drop and heat transfer coefficient varies considerably (see for example Sil500, with a correlation coefficient of 0.886 and 0.986 based on the experimental and numerical data, respectively).

Table 4 summarises the correlation coefficients between the heat transfer coefficients and pressure drops for Case-2.

The results in Table 4 reveal that the heat transfer coefficient-pressure drop correlations differ slightly based on the experimental data for different nanoparticle concentrations (see data of Case-2E). The correlation coefficients between the heat transfer coefficients and pressure drops are unchanging with nanoparticle concentration for the numerically obtained results (see Case-2N* and Case-2N** results, individually). This is due to the fact that both correlations (Gnielinski correlation and Agromayor correlation) induce their own mathematical definitions and trends on the data, resulting in the same $h_{nf} - \Delta p_{nf}$ correlation for varying nanoparticle concentrations. For both cases, the correlation between h_{nf} and Δp_{nf} are very high (<99%), while the 0.994 correlation coefficient values for results using both the Gnielinski correlation and the Agromayor correlation are not of physical significance.

3.6. Statistical assessment, Part 2: Indirect indicators of the nanofluids' heat transfer performance

In this part, we are interested in the relationship between the following parameters: (i) Nu and (Re, Pr, ϕ_v), and (ii) friction factor ξ_{nf} and (Re, ϕ_v) for the metal oxide nanofluid's experimental data by Martínez-Cuenca et al. [29]. Part (i) provides an assessment dominated by a thermal energy point of view, while Part (ii) focuses heavily on the hydrodynamic performance.

The information provided in Tables 5–9 are outputs of standardised statistics tests, and the results are acceptable if and only if such descriptives along with test statistics and p-values are given. Test statistics are indicators of the test relevant for each case (for example, the F-statistics value for ANOVA). In all these cases, the only meaningful indicator is the p-value, as exemplified in the correlation analysis. For the tests we performed, $p \leq 0.05$ leads to a rejection of the hypotheses, while $p > 0.05$ means that the hypotheses should be accepted.

(I) Nu and (Re, Pr, ϕ_v)

The Nusselt number–Reynolds number dataset (as plotted by [29]) is evaluated based on the nanofluid type, nanoparticle concentration, and Prandtl number to quantify these parameters' individual effects. Table 5 shows a comparison of the mean values of Re and Nu, based on the nanofluid type. The traditional (and first) choice in assessment of this task is variance analysis (ANOVA). ANOVA gauges if the mean value of a variable (here, for example, Nu) changes from levels to levels of another variable (here, for example, material type). It assumes that the dependent variable has normal distribution and variances are homogeneous [56]. Since a homogeneity of variances assumption is not valid for the Re dataset, we proceed with the Welch ANOVA test, which does not necessitate homogeneity of variances [57].

Based on the results, it is observed that there is a statistically significant difference between the mean values of Re for the materials

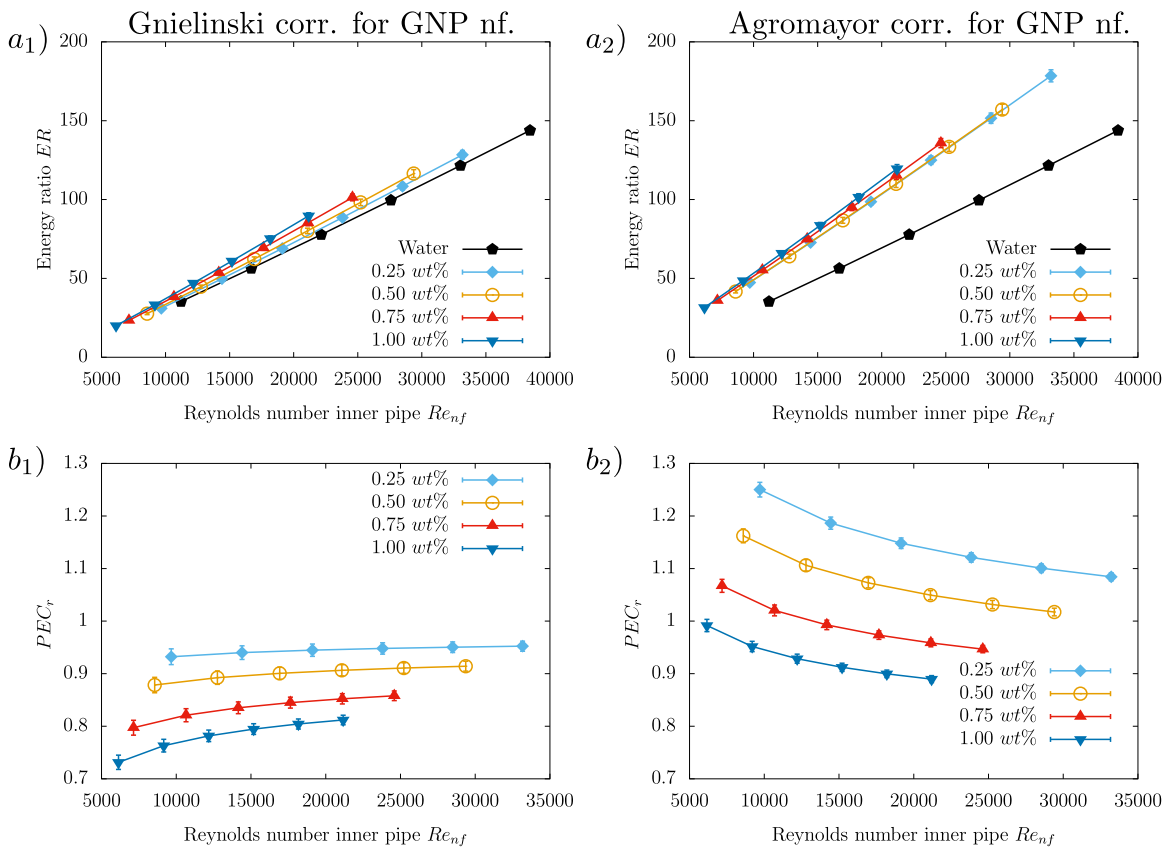

Fig. 9. Expected values and standard deviation of the energy ratio (panels *a*) and PEC ratio (panels *b*) obtained using the Gnielinski correlation [32] and the Agromayor et al. [28] correlation using the SCM method. GNP nanofluid is considered in a pipe-in-pipe heat exchanger.

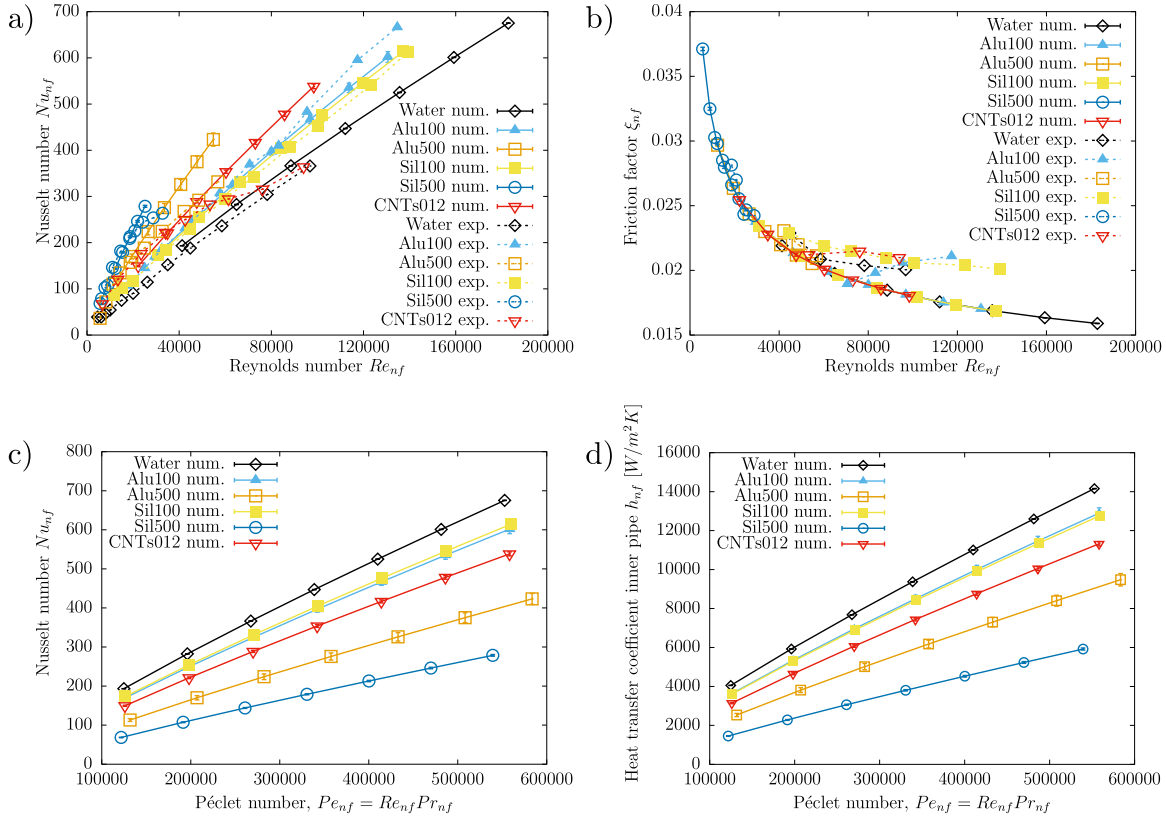

Fig. 10. Comparison of results for the single pipe heat exchanger. Expected values and standard deviation obtained by SCM are shown for (a) Nusselt number and (b) friction factor versus Reynodls number and (c) Nusselt number and (d) heat transfer coefficient versus the Péclet number. Experimental values are taken from Martínez-Cuenca et al. [29].

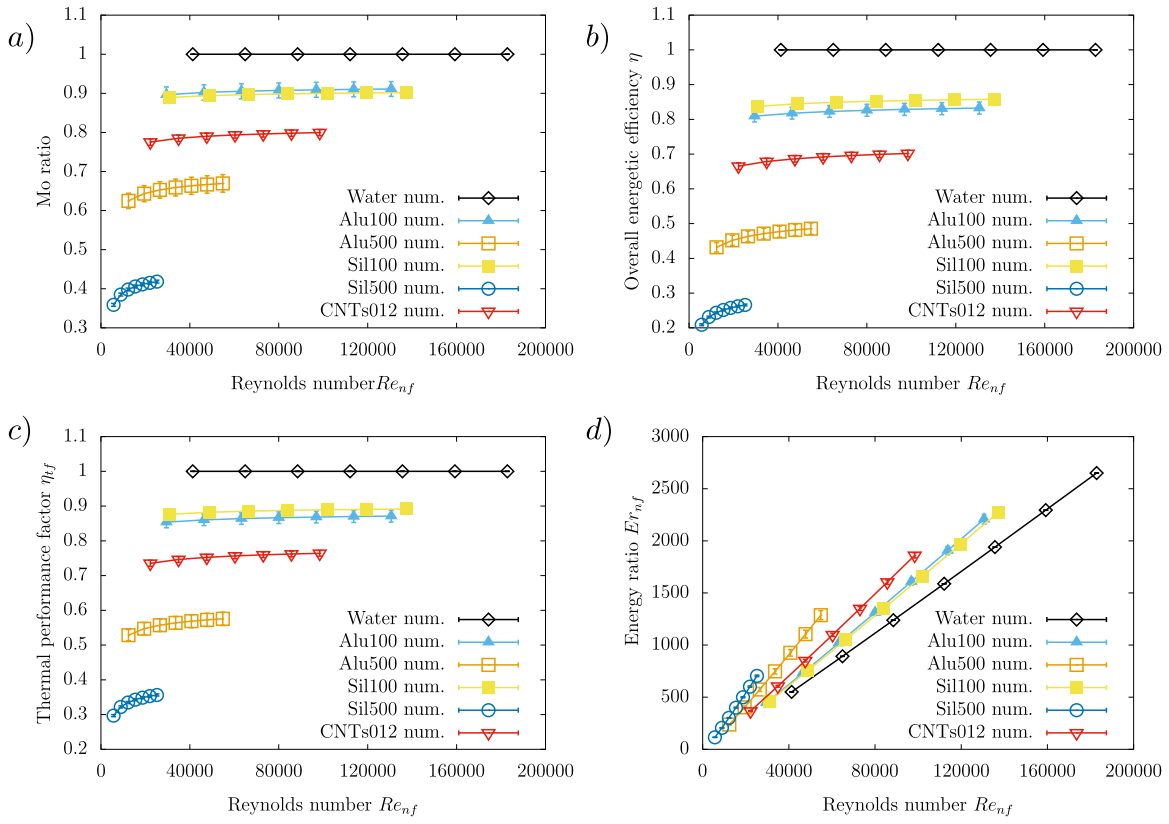

Fig. 11. Comparison of figures of merit for the single pipe heat exchanger. Expected values and standard deviation obtained by SCM are shown for (a) Mouromtseff ratio, (b) overall energetic efficiency, (c) thermal performance factor, and (d) energy ratio.

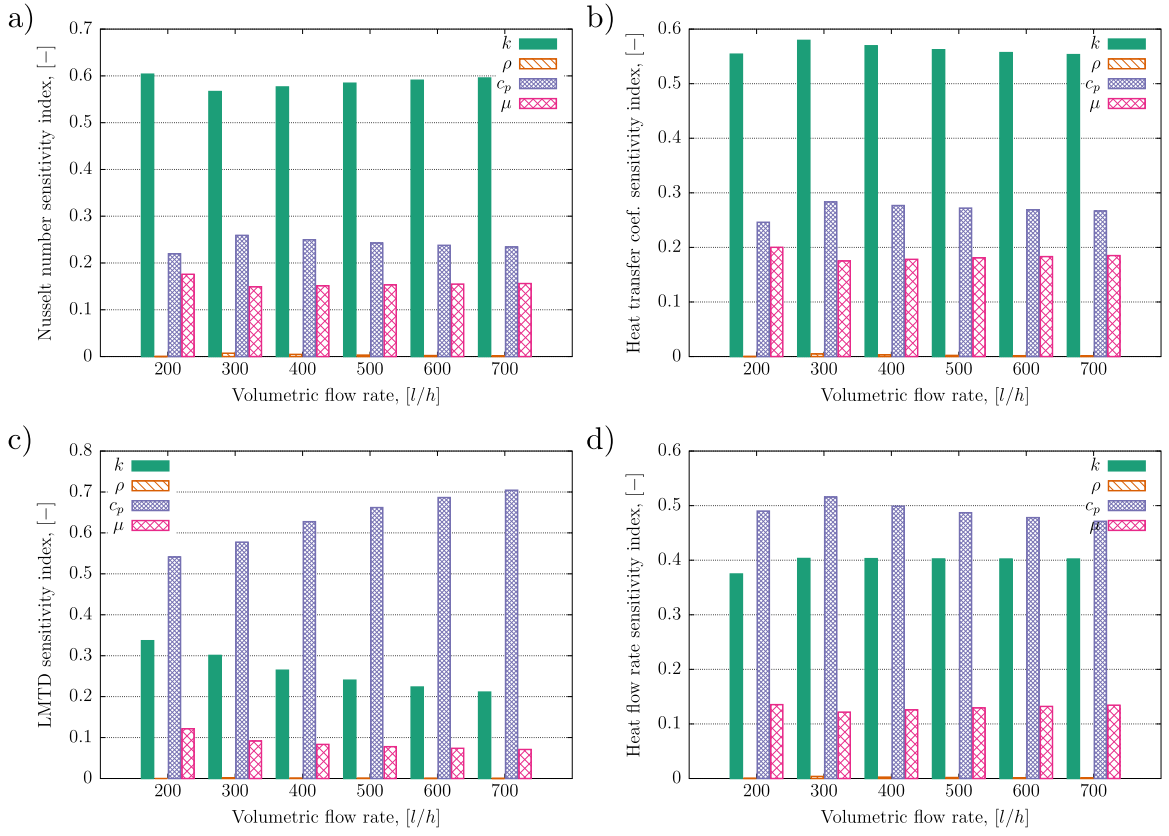

Fig. 12. Sensitivity index compared for (a) Nusselt number, (b) heat transfer coefficient, (c) LMTD and (d) heat flow rate. The results were obtained by analysing the variance for the case of 0.5 wt% GNP nanofluid in the pipe-in-pipe heat exchanger.

Table 5
Comparison of the Re and Nu mean values based on the nanofluid type.

		n	Mean	Standard deviation	Test statistics	p
Re	Alu100	10	67 479	39 961	16.984	0.000*
	Alu500	9	27 752	17 917		
	CNTs012	6	28 878	17 628		
	Sil100	10	69 634	42 503		
	Sil500	8	19 169	8611		
Nu	Alu100	10	351	191	1.875	0.143
	Alu500	9	196	95		
	CNTs012	6	187	83		
	Sil100	10	330	176		
	Sil500	8	205	55		

*$p < 0.05$.

Table 6
Correlation analysis results between ϕ_v, Nu and Re.

	Re		Nu	
	ρ	p	ρ	p
ϕ_v	−0.251	0.73	−215	0.126
Re			0.875	0.000*
Nu				

*$p < 0.05$.

considered ($p < 0.05$). In order to further determine the groups causing this difference, the Post Hoc Bonferroni test (Gerber and Finn [55]) is performed. Results reveal that the mean of Re for Alu100 is different from those of Alu500 and Sil500 ($p = 0.047$ and $p = 0.009$, respectively). The mean Re for Alu100 is higher than the mean Re values of Alu500, and Sil500 groups. The mean Re for Sil100 group is also statistically different from those of Alu500 and Sil500 ($p = 0.029$ and $p = 0.006$, respectively), and the mean Re value of the Sil100 group is higher than those of Alu500 and Sil500.

With respect to the deviation of the mean value of Nu based on the nanofluid type, a further evaluation of Table 5 finds it to be statistically insignificant ($p > 0.05$). This is attributed to the fact that the database consists of nanofluids with average thermal performance with moderate level concentration for metal-oxide and very low concentration for carbon nanotube nanofluid.

Table 6 shows the association between $\phi_v - Nu$, $\phi_v - Re$, and $Nu - Re$ values via the correlation coefficients between these variables. The correlations between $\phi_v - Re$ and $\phi_v - Nu$ are determined to be insignificant ($p > 0.05$) based on the studied dataset. In other words, $\phi_v - Re$ and $\phi_v - Nu$ are not associated in a statistically significant way. This result is due to grouping nanofluids of the same concentration and different type (e.g., Alu500 and Sil500) in this analysis to see the $\phi_v - Re$ and $\phi_v - Nu$ correlations based on the data by [29]. On the other hand, $Re - Nu$ and $Re - Pr$ correlations are statistically significant ($p < 0.05$). The correlation coefficient stands at 0.875 between Re and Nu, indicating a positive and strong relationship. Since an increase in Reynolds number enhances convective transfer of momentum and heat, and since the Nusselt number measures the heat transfer, their statistically significant correlation is expected.

(II) friction factor ξ_{nf} and (Re, ϕ_v)

As in Part I, the dataset does not exhibit homogeneity of variances, and the Welch ANOVA test is used for a comparison of the mean group values of the friction factor, ξ_{nf}. In order to determine of the group(s) causing the difference, the Post Hoc Bonferroni test is used. When $n < 5$, the relation between the variables is controlled using Fisher's Exact test [58].

Table 7 shows the Welch ANOVA test results for the friction factor values depending on the nanofluid type. The mean values of the friction factor are found to be statistically different for different nanofluid types ($p < 0.05$). The mean value of ξ_{nf} for Sil500 was significantly different than those of Alu100, Alu500, CNTs012, and Sil100 groups ($p = 0.000$, $p = 0.001$, $p = 0.000$, and $p = 0.000$, respectively). The mean

Table 7
Comparison of the mean value of friction factor ξ_{nf} based on the nanofluid types.

Material	n	Mean	Standard deviation	Test statistics	p
Alu100	4	0.0202	0.00099	8.289	0.008*
Alu500	3	0.0222	0.00091		
CNTs012	3	0.0213	0.00023		
Sil100	7	0.0213	0.00094		
Sil500	6	0.0272	0.00244		

*$p < 0.05$.

Table 8
Correlation analysis results between friction factor ξ_{nf}, nanoparticle concentration ϕ_v, and Re.

	ξ_{nf}	
	ρ	p
ϕ_v	0.725	0.000*
Re	−0.853	0.000*

*$p < 0.05$.

Table 9
Comparison of the mean value of Nu and friction factor based on the ϕ_v groups.

	ϕ_v(%)	n	Mean	Standard deviation	Test statistics	p
ξ_{nf}	0.125	3	0.0213	0.00023	8.085	0.005*
	1	11	0.0209	0.00106		
	5	9	0.0255	0.00320		
Nu	0.125	6	187	82.7	3.695	0.048*
	1	29	298	177		
	5	17	201	76.5		

*$p < 0.05$.

friction factor value for Sil500 group is higher than those of Alu100, Alu500, CNTs012, and Sil100 groups. Hence, it can be inferred that this difference is caused by the Sil500 group in the dataset. The correlations between ξ_{nf}, ϕ_v, and Re are summarised in Table 8. The correlation coefficients in Table 8 are Pearson correlation coefficients since the data exhibit normal distribution.

The correlation between ϕ_v and ξ_{nf} is statistically significant ($p < 0.05$) with a coefficient of 0.725, which shows a positive and strong association. The correlation between ξ_{nf} and Re is significant ($p < 0.05$) with an even greater correlation coefficient value, i.e., −0.853, showing a negative and strong relation. The friction factor represents a transfer of momentum from the fluid to the pipe walls and as such depends on the surface roughness of the wall and on the Reynolds number. Therefore, Re and ξ_{nf} are expected to be strongly correlated. Furthermore, since nanoparticle volume fraction influences the fluid viscosity and thus the Reynolds number, the statistically significant correlation between ϕ_v and ξ_{nf} is also expected.

The final assessment is based on the effect of the nanoparticle loading on Nu and ξ_{nf}. This is one of the fundamental dependences of the thermal phenomena on the nanofluid structure. Timofeeva et al. [59] stated that the heat transfer coefficient and the pumping power penalty are strongly dependent on the nanoparticle concentration of nanofluids. Since the heat transfer coefficient and the pumping power penalty are optimised as "the higher the better" and "the lower the better", respectively [59], and both are positively dependent on the nanoparticle concentration, this presents an optimisation problem for engineers: "how to increase the heat transfer performance without too much increasing the pumping power requirement?" In tackling this problem, the results presented in Table 9 are insightful as they reflect the change in the mean values of Nu and ξ_{nf} based on the nanoparticle concentration.

Here the aim is to test whether there is a difference in the mean values of Nu and ξ_{nf} based on the nanoparticle concentration. For this purpose, the Welch ANOVA test is used. The results show that the mean values of ξ_{nf} and Nu differ between the ϕ_v groups (both $p < 0.05$). In

order to determine the group or groups causing such differences, the Post Hoc Bonferroni test is applied. For friction factor trends, the results showed that the mean value of ξ_{nf} for group 5 is different than those of group 1 and group 0.125 in a statistically significant way ($p = .000$ and $p = .025$, respectively). It can be said that the mean value of ξ_{nf} is greater for group 5 compared against those of groups 1 and 0.125. When it comes to determination of the group or groups causing the difference in Nu trends, the Post Hoc Bonferroni test did not identify any specific group. This is due to the high standard deviations, although the mean values of Nu with respect to ϕ_v groups are considerably different.

4. Conclusions

The use of the Stochastic Collocation Method with a large number of deterministic simulations allows the uncertainty to be transferred from the model parameters to the simulation results. In this paper, we have considered the experimental uncertainty of thermal conductivity, viscosity, specific heat, and density of various nanofluids as model parameters. Using empirical correlations, we developed a deterministic algorithm for estimating the heat transfer performance of the heat exchanger with nanofluid flowing through inner pipe in a turbulent flow regime ($Re \approx 4{,}000{-}180{,}000$). The algorithm was used with the SCM to evaluate the expected values and variance of the Nusselt number, friction factor, and other performance indicators of the heat exchanger. We have found that in most cases the variances in estimating heat exchanger performance are so small that the conclusions drawn from a deterministic simulation of a heat exchanger are valid. The deviations determined are of the same order of magnitude as those caused by the change in the volume fraction of the nanoparticles by 0.25%.

Furthermore, we confirmed that uncertainty in thermal conductivity, specific heat, and viscosity have a larger impact on the performance indicators of the heat exchanger, while the uncertainty in density is less important. If future studies are made, density can be considered as a known parameter and its uncertainty neglected.

To estimate the heat transfer in a heat exchanger, we compared two types of empirical correlations: the well-known Gnielinski correlation, which was developed for pure fluids, and a correlation specifically tailored to a particular nanofluid and heat exchanger. The results show that the correlations developed for pure fluids should be used with caution when modelling nanofluids with effective thermophysical properties as the results differ significantly. This is specially true for graphene nanoplatelets nanofluid and for nanofluids with higher concentrations of nanoparticles in heat exchangers operating at high Reynolds numbers. The results and the SCM variance obtained with the specially tailored correlation are within the error limits of the experimental measurements, while the use of the general Gnielinski correlation leads to a significant underestimation of the heat transfer.

The statistical assessment of this work aims at quantitatively discussing the thermal conductivity enhancement and pressure loss relationships by considering a wide range of nanofluid types (metal-oxide, carbon nanotube, and graphene nanoplatelet nanoparticles dispersions) from the literature. For this purpose, experimental data from [28,29] are processed along with the data from the numerical simulations of this current work. Statistical assessment consists of correlation analysis to uncover the level of association between two key variables, one of which is desired to be maximised and the other is desired to be kept as low as possible, i.e., heat transfer coefficient and pressure drop, respectively. The results (in Part 1, Section 3.5) show that these variables are strongly correlated with each other and they are directly proportional. Hence, the optimisation problem of maximising the heat transfer coefficient whilst keeping the pressure losses low is a large-scale challenge, starting with nanofluid formulation and including the heat transfer setup settings. When numerically simulated, the results implicitly include the mathematical dependences induced by the heat transfer correlations used, and thereby the correlation coefficients are very close (if not the same) for the nanofluids considered. The results in Part 2 (Section 3.6) reveal that the nanoparticle concentration-Nu relationship is statistically insignificant based on the studied dataset, while the $Re - Nu$ relation is significant, pointing out the importance of flow conditions. While the nanoparticle concentration-Nu relationship is statistically insignificant, the nanoparticle concentration-friction factor correlation is significant and strong. This outcome points to the conclusion that the thermal-hydrodynamic behaviour optimisation should be sought in a parameter other than nanoparticle fraction.

Declaration of competing interest

The authors declare that they have no known competing financial interests or personal relationships that could have appeared to influence the work reported in this paper.

Acknowledgements

This article is based upon work from COST Innovators Grant IG15119 Nanoconvex (Nanofluids for convective heat transfer devices), supported by COST (European Cooperation in Science and Technology).

References

[1] S.U.S. Choi, Enhancing thermal conductivity of fluids with nanoparticles, Dev. Appl. Non Newton. Flows 66 (1995) 99–106.

[2] B.C. Pak, Y.I. Cho, Hydrodynamic and heat transfer study of dispersed fluids with submicron metallic oxide particles, Exp. Heat Transfer 11 (1998) 151–170.

[3] M.H. Buschmann, R. Azizian, T. Kempe, J.E. Juliá, R. Martínez-Cuenca, B. Sundén, Z. Wu, A. Seppälä, T. Ala-Nissila, Correct interpretation of nanofluid convective heat transfer, Int. J. Therm. Sci. 129 (June 2017) (2018) 504–531, http://dx.doi.org/10.1016/j.ijthermalsci.2017.11.003.

[4] E. Abu-Nada, Effects of variable viscosity and thermal conductivity of Al_2O_3-water nanofluid on heat transfer enhancement in natural convection, Int. J. Heat Fluid Flow 30 (4) (2009) 679–690, http://dx.doi.org/10.1016/j.ijheatfluidflow.2009.02.003.

[5] A.T. Utomo, E.B. Haghighi, A.I. Zavareh, M. Ghanbarpourgeravi, H. Poth, R. Khodabandeh, B. Palm, A.W. Pacek, The effect of nanoparticles on laminar heat transfer in a horizontal tube, Int. J. Heat Mass Transfer 69 (2014) 77–91, http://dx.doi.org/10.1016/j.ijheatmasstransfer.2013.10.003.

[6] M. Awais, A.A. Bhuiyan, S. Salehin, M.M. Ehsan, B. Khan, M.H. Rahman, Synthesis, heat transport mechanisms and thermophysical properties of nanofluids: A critical overview, Int. J. Thermofluids 10 (2021) 100086, http://dx.doi.org/10.1016/j.ijft.2021.100086, URL https://www.sciencedirect.com/science/article/pii/S2666202721000240.

[7] M.M. Ali, R. Akhter, M. Miah, Hydromagnetic mixed convective flow in a horizontal channel equipped with Cu-water nanofluid and alternated baffles, Int. J. Thermofluids 12 (2021) 100118, http://dx.doi.org/10.1016/j.ijft.2021.100118, URL https://www.sciencedirect.com/science/article/pii/S2666202721000562.

[8] T. Salameh, P.P. Kumar, E.T. Sayed, M.A. Abdelkareem, H. Rezk, A. Olabi, Fuzzy modeling and particle swarm optimization of Al2O3/SiO2 nanofluid, Int. J. Thermofluids 10 (2021) 100084, http://dx.doi.org/10.1016/j.ijft.2021.100084, URL https://www.sciencedirect.com/science/article/pii/S2666202721000227.

[9] P. Barnoon, Numerical assessment of heat transfer and mixing quality of a hybrid nanofluid in a microchannel equipped with a dual mixer, Int. J. Thermofluids 12 (2021) 100111, http://dx.doi.org/10.1016/j.ijft.2021.100111, URL https://www.sciencedirect.com/science/article/pii/S2666202721000495.

[10] E. Cuce, P.M. Cuce, T. Guclu, A.B. Besir, On the use of nanofluids in solar energy applications, J. Therm. Stresses 29 (3) (2020) 513–534, http://dx.doi.org/10.1007/s11630-020-1269-3, URL http://link.springer.com/10.1007/s11630-020-1269-3.

[11] Z. Guo, A review on heat transfer enhancement with nanofluids, J. Enhanced Heat Transf. 27 (1) (2020) 1–70, http://dx.doi.org/10.1615/JEnhHeatTransf.2019031575.

[12] I. Gonçalves, R. Souza, G. Coutinho, J.a. Miranda, A. Moita, J.E. Pereira, A. Moreira, R. Lima, Thermal conductivity of nanofluids: A review on prediction models, controversies and challenges, Appl. Sci. 11 (6) (2021) 2525, http://dx.doi.org/10.3390/app11062525, URL https://www.mdpi.com/2076-3417/11/6/2525.

[13] E.B. Elcioglu, A. Guvenc Yazicioglu, A. Turgut, A.S. Anagun, Experimental study and taguchi analysis on alumina-water nanofluid viscosity, Appl. Therm. Eng. 128 (2018) 973–981, http://dx.doi.org/10.1016/j.applthermaleng.2017.09.013, URL https://linkinghub.elsevier.com/retrieve/pii/S1359431116339941.

[14] S. Iranmanesh, M. Mehrali, E. Sadeghinezhad, B.C. Ang, H.C. Ong, A. Esmaeilzadeh, Evaluation of viscosity and thermal conductivity of graphene nanoplatelets nanofluids through a combined experimental–statistical approach using respond surface methodology method, Int. Commun. Heat Mass Transfer 79 (2016) 74–80, http://dx.doi.org/10.1016/j.icheatmasstransfer.2016.10.004, URL https://linkinghub.elsevier.com/retrieve/pii/S0735193316303025.

[15] B. Everitt, A. Skrondal, The Cambridge Dictionary of Statistics, fourth ed., Cambridge University Press, 2010, p. 23.

[16] P.Y. Chen, P.M. Popovich, Correlation: Parametric and nonparametric measures, in: Correlation, SAGE Publications, Inc., 2455 Teller Road, Thousand Oaks California 91320 United States of America, 2011, pp. 2–87, http://dx.doi.org/10.4135/9781412983808.n1, URL http://srmo.sagepub.com/view/correlation/n1.xml.

[17] E. Elcioglu, B. Kamenik, A. Turgut, R. Mondragon, L. Hernandez Lopez, J. Vallejo, L. Lugo, M. Buschmann, J. Ravnik, Graphene nanoplatelet nanofluids thermal and hydrodynamic performances revisited, in: 3rd European Symposium on Nanofluids (ESNf), 2021.

[18] E.B. Elcioglu, A high-accuracy thermal conductivity model for water-based graphene nanoplatelet nanofluids, Energies 14 (16) (2021) 5178, http://dx.doi.org/10.3390/en14165178, URL https://www.mdpi.com/1996-1073/14/16/5178.

[19] S. Porgar, L. Vafajoo, N. Nikkam, G.V. Nezhaad, Physiochemical studies of functionalized MWCNT/transformer oil nanofluid utilized in a double pipe heat exchanger, Can. J. Chem. 99 (6) (2021) 510–518, http://dx.doi.org/10.1139/cjc-2020-0297, URL https://cdnsciencepub.com/doi/10.1139/cjc-2020-0297.

[20] J. Avsec, M. Oblak, The calculation of thermal conductivity, viscosity and thermodynamic properties for nanofluids on the basis of statistical nanomechanics, Int. J. Heat Mass Transfer 50 (21–22) (2007) 4331–4341, http://dx.doi.org/10.1016/j.ijheatmasstransfer.2007.01.064.

[21] V.Y. Rudyak, A. Minakov, M. Pryazhnikov, Preparation, characterization, and viscosity studding the single-walled carbon nanotube nanofluids, J. Molecular Liquids 329 (2021) 115517, http://dx.doi.org/10.1016/j.molliq.2021.115517, URL https://linkinghub.elsevier.com/retrieve/pii/S0167732221002439.

[22] R. Feng, Improving uncertainty analysis in well log classification by machine learning with a scaling algorithm, J. Pet. Sci. Eng. 196 (2021) 107995, http://dx.doi.org/10.1016/j.petrol.2020.107995, URL https://linkinghub.elsevier.com/retrieve/pii/S0920410520310500.

[23] P. Pitchai, N.K. Jha, R.G. Nair, P. Guruprasad, A coupled framework of variational asymptotic method based homogenization technique and Monte Carlo approach for the uncertainty and sensitivity analysis of unidirectional composites, Compos. Struct. 263 (2021) 113656, http://dx.doi.org/10.1016/j.compstruct.2021.113656, URL https://linkinghub.elsevier.com/retrieve/pii/S0263822321001173.

[24] X. Jiang, S. Li, R. Furfaro, Z. Wang, Y. Ji, High-dimensional uncertainty quantification for mars atmospheric entry using adaptive generalized polynomial chaos, Aerosp. Sci. Technol. 107 (2020) 106240, http://dx.doi.org/10.1016/j.ast.2020.106240, URL https://linkinghub.elsevier.com/retrieve/pii/S1270963820309226.

[25] W. Kun, C. Fu, Y. Jianyang, S. Yanping, Nested sparse-grid stochastic collocation method for uncertainty quantification of blade stagger angle, Energy 201 (2020) 117583, http://dx.doi.org/10.1016/j.energy.2020.117583, URL https://linkinghub.elsevier.com/retrieve/pii/S0360544220306903.

[26] J. Ravnik, M. Ramšak, M. Zadravec, B. Kamenik, M. Hriberšek, Experimental and stochastic analysis of lyophilisation, Eur. J. Pharmaceut. Biopharmaceut. 159 (2021) 108–122, http://dx.doi.org/10.1016/j.ejpb.2020.12.011, URL https://linkinghub.elsevier.com/retrieve/pii/S0939641120303696.

[27] S. Razavi, A. Jakeman, A. Saltelli, C. Prieur, B. Iooss, E. Borgonovo, E. Plischke, S.L. Piano, T. Iwanaga, W. Becker, et al., The future of sensitivity analysis: an essential discipline for systems modeling and policy support, Environ. Model. Softw. 137 (2021) 104954.

[28] R. Agromayor, D. Cabaleiro, A. Pardinas, J. Vallejo, J. Fernandez-Seara, L. Lugo, Heat transfer performance of functionalized graphene nanoplatelet aqueous nanofluids, Materials 9 (6) (2016) 455, http://dx.doi.org/10.3390/ma9060455, URL http://www.mdpi.com/1996-1944/9/6/455.

[29] R. Martínez-Cuenca, R. Mondragón, L. Hernández, C. Segarra, J.C. Jarque, T. Hibiki, J.E. Juliá, Forced-convective heat-transfer coefficient and pressure drop of water-based nanofluids in a horizontal pipe, Appl. Therm. Eng. 98 (2016) 841–849, http://dx.doi.org/10.1016/j.applthermaleng.2015.11.050.

[30] R. Mondragón, C. Segarra, R. Martínez-Cuenca, J.E. Juliá, J.C. Jarque, Experimental characterization and modeling of thermophysical properties of nanofluids at high temperature conditions for heat transfer applications, Powder Technol. 249 (2013) 516–529, http://dx.doi.org/10.1016/j.powtec.2013.08.035.

[31] M. Pavía, K. Alajami, P. Estellé, A. Desforges, B. Vigolo, A critical review on thermal conductivity enhancement of graphene-based nanofluids, Adv. Colloid Interface Sci. 294 (2021) 102452, http://dx.doi.org/10.1016/j.cis.2021.102452, URL https://linkinghub.elsevier.com/retrieve/pii/S0001868621000932.

[32] V.V. Gnielinski, Neue gleichungen fuer den waerme- und den stoffuebergang in turbulent durchstroemten rohren und kanaelen, Forsch. Ing.-Wes. 41 (1) (1975) 8–16.

[33] F.P. Incropera, Fundamentals of Heat and Mass Transfer, John Wiley & Sons, Inc., Hoboken, NJ, USA, 2006.

[34] V. Gnielinski, Heat transfer in concentric annular and parallel plate ducts, in: VDI Heat Atlas, 2010, pp. 701–708.

[35] C.J. Ho, J.-C. Liao, C.-H. Li, W.-M. Yan, M. Amani, Experimental study of cooling characteristics of water-based alumina nanofluid in a minichannel heat sink, Case Stud. Therm. Eng. 14 (2019) 100418.

[36] I.M. Mahbubul, E.B. Elcioglu, M.A. Amalina, R. Saidur, Stability, thermophysical properties and performance assessment of alumina–water nanofluid with emphasis on ultrasonication and storage period, Powder Technol. 345 (2019) 668–675.

[37] L. Yu, D. Liu, Study of the thermal effectiveness of laminar forced convection of nanofluids for liquid cooling applications, IEEE Trans. Compon. Packag. Manuf. Technol. 3 (10) (2013) 1693–1704.

[38] A. Datta, P. Halder, Thermal efficiency and hydraulic performance evaluation on $Ag - Al_2O_3$ and $SiC - Al_2O_3$ hybrid nanofluid for circular jet impingement, Arch. Thermodyn. 42 (1) (2021).

[39] N.P. Devi, C.S. Rao, K.K. Kumar, Thermal performance of nanofluids in heat transfer loops, in: IOP Conference Series: Materials Science and Engineering, Vol. 981, IOP Publishing, 2020, p. 42029.

[40] S.-H. Lee, H.J. Kim, S.P. Jang, Thermal performance criterion for nanofluids in laminar flow regime, J. Mech. Sci. Technol. 31 (2) (2017) 975–983.

[41] Z. Wu, L. Wang, B. Sundén, Pressure drop and convective heat transfer of water and nanofluids in a double-pipe helical heat exchanger, Appl. Therm. Eng. 60 (1–2) (2013) 266–274.

[42] E.B. Elcioglu, A.M. Genc, Z.H. Karadeniz, M.A. Ezan, A. Turgut, Nanofluid figure-of-merits to assess thermal efficiency of a flat plate solar collector, Energy Convers. Manage. 204 (November 2019) (2020) 112292, http://dx.doi.org/10.1016/j.enconman.2019.112292.

[43] A.A. Minea, Comparative study of turbulent heat transfer of nanofluids, J. Therm. Anal. Calorim. 124 (1) (2016) 407–416.

[44] A.E. Bergles, A. Bar-Cohen, Direct liquid cooling of microelectronic components, Adv. Therm. Model. Electron. Compon. Syst. 2 (1990) 233–342.

[45] G. Sekrani, S. Poncet, P. Proulx, Modeling of convective turbulent heat transfer of water-based Al_2O_3 nanofluids in an uniformly heated pipe, Chem. Eng. Sci. 176 (2018) 205–219.

[46] R.S. Vajjha, D.K. Das, A review and analysis on influence of temperature and concentration of nanofluids on thermophysical properties, heat transfer and pumping power, Int. J. Heat Mass Transfer 55 (15–16) (2012) 4063–4078.

[47] R. Agromayor, D. Cabaleiro, A.A. Pardinas, J.P. Vallejo, J. Fernandez-Seara, L. Lugo, Heat transfer performance of functionalized graphene nanoplatelet aqueous nanofluids, Materials 9 (6) (2016) http://dx.doi.org/10.3390/ma9060455.

[48] S. Smolyak, Quadrature and interpolation formulas for tensor products of certain classes of functions, Sov. Math. Dokl. 4 (1963) 240–243.

[49] F. Nobile, R. Tempone, C.G. Webster, A sparse grid stochastic collocation method for partial differential equations with random input data, SIAM J. Numer. Anal. 46 (5) (2008) 2309–2345, http://dx.doi.org/10.1137/060663660, URL http://epubs.siam.org/doi/10.1137/060663660.

[50] A. Šušnjara, O. Verhnjak, D. Poljak, M. Cvetković, J. Ravnik, Stochastic-deterministic boundary element modelling of transcranial electric stimulation using a three layer head model, Eng. Anal. Bound. Elem. 123 (2021) 70–83, http://dx.doi.org/10.1016/j.enganabound.2020.11.010, URL https://linkinghub.elsevier.com/retrieve/pii/S0955799720302939.

[51] P. Keblinski, J.A. Eastman, D.G. Cahill, Nanofluids for thermal transport, Mater. Today 8 (6) (2005) 36–44.

[52] U. Calviño, J.P. Vallejo, M.H. Buschmann, J. Fernández-seara, L. Lugo, Analysis of heat transfer characteristics of a GnP aqueous nanofluid through a double-tube heat exchanger, Nanomaterials 11 (4) (2021) http://dx.doi.org/10.3390/nano11040844.

[53] S. Tschisgale, T. Kempe, Deterioration of heat transfer in turbulent channel flows due to nanoparticles, Int. J. Heat Mass Transfer 175 (2021) 121392, http://dx.doi.org/10.1016/j.ijheatmasstransfer.2021.121392.

[54] A. Saltelli, M. Ratto, T. Andres, F. Campolongo, D. Gatelli, M. Saisana, S. Tarantola, Global Sensitivity Analysis: The Primer, John Wiley and sons, Ltd, West Susex, England, 2008.

[55] S.B. Gerber, K.V. Finn, Using SPSS for Windows: Data Analysis and Graphics, Springer, 2013.

[56] M. Delacre, C. Leys, Y.L. Mora, D. Lakens, Taking parametric assumptions seriously: Arguments for the use of Welch's F-test instead of the classical F-test in one-way ANOVA, Int. Rev. Soc. Psychol. 32 (1) (2019).

[57] H. Liu, Comparing Welch ANOVA, a Kruskal-Wallis Test, and Traditional ANOVA in Case of Heterogeneity of Variance, Virginia Commonwealth University, 2015.

[58] G.J. Upton, Fisher'S exact test, J. R. Statist. Soc.: Ser. A 155 (3) (1992) 395–402.

[59] E.V. Timofeeva, Nanofluids for heat transfer – potential and engineering strategies, in: A. Ahsan (Ed.), Two Phase Flow, Phase Change and Numerical Modeling, IntechOpen, Rijeka, 2011, http://dx.doi.org/10.5772/22158.